104 (2025) 105020

Contents lists available at ScienceDirect

Poultry Science

journal homepage: www.elsevier.com/locate/psj

Full-Length Article

Liver transcriptome response to avian pathogenic *Escherichia coli* infection in broilers with corticosterone treatment

Mengru Chen [a,b], Yifei He [a,b], Yimin Jia [a,b], Lei Wu [a,b], Ruqian Zhao [a,b,*]

[a] MOE Joint International Research Laboratory of Animal Health & Food Safety, Nanjing Agricultural University, Nanjing, Jiangsu, 210095, PR China
[b] Key Laboratory of Animal Physiology & Biochemistry, College of Veterinary Medicine, Nanjing Agricultural University, Nanjing, Jiangsu, 210095, PR China

ARTICLE INFO

Keywords:
Avian pathogenic *Escherichia coli*
Stress
Liver
Immunity
Lipid metabolism

ABSTRACT

Avian pathogenic *Escherichia coli* (**APEC**) infection has high morbidity and mortality, and multiple stressors encountered during rearing place poultry in a state of stress. However, research on how poultry cope with APEC infection under stress situation is still limited. In this study, we established a broiler stress model by corticosterone (**CORT**) administration subcutaneously for 7 consecutive days, followed by APEC challenge intramuscularly. CORT treatment significantly reduced body weight (**BW**) and average daily gain (**ADG**) while increasing feed conversion ratio (**FCR**) ($P < 0.01$). APEC infection significantly decreased ADG ($P < 0.01$). CORT treatment and APEC infection elevated plasma corticosterone and heterophil to lymphocyte (**H/L**) ratio ($P < 0.05$). Additionally, plasma aspartate aminotransferase (**AST**), AST to alanine aminotransferase (**AST/ALT**) ratio, and lactate dehydrogenase (**LDH**) levels increased significantly ($P < 0.01$). Histopathological analysis revealed structural damage of liver, indicating that CORT treatment and APEC infection induced liver injury. However, CORT pretreatment broilers exhibited a milder histopathological lesions and significantly lower AST, ALT, and LDH levels ($P < 0.05$) compared to APEC infection alone. CORT treatment and APEC infection increased plasma levels of lysozyme (**LZM**), total protein (**TP**), and globulin (**GLOB**) ($P < 0.05$), while CORT pretreatment further elevating their concentrations compared to APEC infection alone, suggesting an enhanced innate immune response. Liver transcriptomic analysis identified 768, 335, and 567 differentially expressed genes (**DEGs**) following CORT, APEC, or both treatments, respectively, enriched in cytokine-cytokine receptor interaction, PPAR signaling pathway, Toll-like receptor signaling pathway, MAPK signaling pathway, steroid hormone biosynthesis pathway, arachidonic acid metabolism, and phagosome pathway, etc., indicating that CORT treatment regulates lipid metabolism and immunity, while APEC infection induces inflammation and disrupts lipid metabolism. Notably, CORT pretreatment may mitigate APEC induced liver injury by enhancing phagosome function. Moreover, glucocorticoid receptor (**GR**) may regulate DEGs expressions, thus affected broilers response to CORT, APEC, or both treatments. These results suggest that CORT treatment, APEC infection, or both significantly affect the growth performance, immune response and liver function of broilers, while lipid metabolism may play a crucial role.

Introduction

Avian pathogenic *Escherichia coli* (**APEC**) is a common pathogen in birds that causes avian colibacillosis globally, leading to substantial economic losses in the poultry industry (Kathayat et al., 2021; Ha et al., 2023). As an important subtype of extraintestinal pathogenic *Escherichia coli* (**ExPEC**), APEC can cause a variety of localized and systemic infections in poultry of different ages and breeds, resulting in high morbidity and mortality rates (Kathayat et al., 2021; Helmy et al., 2022). APEC invades the host through specific virulence factors, such as adhesins, invasins, protectins and iron acquisition systems, and evades the host's immune response, thereby causing clinical symptoms, such as pericarditis, salpingitis, peritonitis, perihepatitis and septicemia (Dziva and Stevens, 2008; Hu et al., 2022). Studies have shown that different geographic regions harbor distinct prevalent serotypes, with O1, O2 and O78 being the predominant serotypes of APEC, and the detection rates of other serotypes, such as O5, O18 and O35, have also increased (Mehat et al., 2021). In addition to posing a threat to poultry health, APEC is

* Corresponding author at: MOE Joint International Research Laboratory of Animal Health & Food Safety; Key Laboratory of Animal Physiology & Biochemistry, College of Veterinary Medicine, Nanjing Agricultural University, Nanjing, Jiangsu, 210095, PR China.
E-mail address: zhaoruqian@njau.edu.cn (R. Zhao).

https://doi.org/10.1016/j.psj.2025.105020
Received 2 January 2025; Accepted 10 March 2025
Available online 10 March 2025

also a potential zoonotic pathogen with foodborne transmission. Humans can contract urinary tract infections and meningitis through the consumption of contaminated poultry products, severely endanger human health (Mellata, 2013). For example, APEC O18 isolates can survive in human serum, cause meningitis in mice through pathogenic mechanism similar to that of Neonatal meningitis *Escherichia coli* (**NMEC**) strains, and induce neuronal apoptosis (Krishnan et al., 2015).

Perihepatitis is a characteristic symptom observed in poultry after APEC infection, resulting in liver damage (Hu et al., 2022; Meng et al., 2024). Liver, as the largest metabolic organ in the body, plays an important role not only in substance metabolism, energy metabolism and digestion, but also serve as a unique immune organ, playing a crucial role in immune response (Heymann and Tacke, 2016). The liver eliminates pathogens through innate immune cells, including Kupffer cells, dendritic cells, and natural killer cells, and T cells and B cells participate in adaptive immunity (Robinson et al., 2016). There is an interaction between liver metabolism and immunity, and it is particularly evident in disease states. Studies have shown that in non-alcoholic fatty liver disease (**NAFLD**), metabolic stress can activate immune cells, ultimately promoting the development of liver inflammation and fibrosis (Guo et al., 2024). Our previous studies have shown that stress altered liver lipid metabolism in broilers, leading to lipid deposition in the liver (Liu et al., 2024). However, the impact of this change on broilers' response to pathogen infection is still unclear.

Stress is an adaptive response after the stressor stimulates the body and is accompanied by the activation of the neuroendocrine network (Chrousos and Gold, 1992). In response to stress, the hypothalamic-pituitary-adrenal (**HPA**) axis is activated, leading to the release of glucocorticoid from the adrenal cortex, which regulates the stress response by binding to glucocorticoid receptor (**GR**) (Gjerstad et al., 2018). As a nuclear transcription factor, GR regulates gene transcription by binding to glucocorticoid response elements (**GRE**) in the promoter regions of target genes (Bekhbat et al., 2017). Previous studies have shown that under stress status, GR regulates the expression of lipogenesis-related genes, influencing hepatic lipid metabolism and resulting in lipid deposition in the liver (Hu et al., 2018). In the process of breeding, poultry will be stimulated by a variety of stressors, including environment, nutrition, feeding management, and pathogens, which have a great impact on production performance. Studies have shown that chronic heat stress can reduce feed intake of broilers, increase feed conversion ratio (**FCR**), reduce growth rate, and ultimately affect economic benefits (Mohammed et al., 2019; Liu et al., 2023). Moreover, the immune function of poultry is also affected. For example, chronic heat stress can increase the heterophil to lymphocyte (**H/L**) ratio in broilers (Kim et al., 2021), change the intestinal microbiota, and lead to intestinal damage and pathogen translocation (Mohammed et al., 2019; Jiang et al., 2021). In addition, dexamethasone (**DEX**) treatment can lead to a decrease in bursa of Fabricius weight in broilers (Islam et al., 2023). However, research on how poultry to cope with pathogen infection and what role GR plays under stress situation is still limited.

Current research primarily focus on the individual effects of stress and APEC infection on poultry. However, it is still unclear how poultry respond to APEC infection under stress status. Therefore, the purpose of this study is to investigate the effects of stress, APEC infection, and their combination on poultry growth performance, immune response and liver function.

Materials and methods

Ethical statement

The animal experiment was approved by the Institutional Animal Care and Use Committee of Nanjing Agricultural University according to the Guidelines on Ethical Treatment of Experimental Animals (2006) No. 398 set by the Ministry of Science and Technology (2006, Beijing, China). The project number is NJAU.No20240517094.

Avian pathogenic Escherichia coli O18 culture

The avian pathogenic *Escherichia coli* O18 strain was provided by Jiangsu Lihua Animal Husbandry Co., LTD.. The bacterial inocula were prepared by 24 h of growth on Luria-Bertani (**LB**) broth at 37 °C. The bacteria counts were adjusted to 5×10^6 CFU/mL to get sufficient bacteria for intramuscular injection to broilers.

Corticosterone solution preparation

Corticosterone (**CORT**) (Shanghai Aladdin Biochemical Technology Co., Ltd., C104537, Shanghai, China) was first dissolved with anhydrous ethanol and then diluted with normal saline into a 15 % ethanol-saline solution. The corticosterone solution was stored at 4 °C for later use.

Experimental design and treatment

A total of 44 1-day-old male Arbor Acres broilers (Jiangsu Jinghai Poultry Industry Co., Ltd., Jiangsu, China) were raised in the environmental control warehouse of Nanjing Agricultural University. Broilers were raised in strict accordance with the Arbor Acres broiler feeding manual. After 3 days of adaptive feeding, all broilers were randomly divided into 4 groups: control group (**CON**), CORT-treated group (**CORT**), control and *Escherichia coli* infection group (**CON + *E.coli***), CORT-treated and *Escherichia coli* infection group (**CORT + *E.coli***), with 11 broilers per group. From day 22, all broilers were weighed daily. The broilers in CORT group and CORT + *E. coli* group were injected subcutaneously with corticosterone solution (4 mg/kg), while those in the CON group and CON + *E. coli* group were administered with the ethanol-saline solution. This treatment was conducted for 7 consecutive days. On day 29, broilers in CON + *E.coli* group and CORT + *E.coli* group were intramuscularly injected with 0.2 mL 5×10^6 CFU/mL *Escherichia coli* inoculum, while CON group and CORT group were injected with an equal volume of saline. The experimental flow chart was shown in Fig. 1A. All broilers were kept at a stable ambient temperature of 33 to 35 °C for the first 3 days, then decreased by 3 °C per week. A light cycle of 23 h of light and 1 h of darkness(**23L: 1D**) during the first week, 20L: 4D during the 2 to 4weeks, and 23L: 1D until the end of the experiment were implemented. Ambient humidity was controlled at 40 % to 60 % throughout the experimental period. The nutritional composition of the diets used in the study is shown in Table 1. All the broilers had free access to water and feed throughout the experiment.

Growth performance

Body weight (**BW**) and feed intake were measured before and 24 h after *Escherichia coli* infection, then average daily weight gain (**ADG**), average daily feed intake (**ADFI**) and feed conversion ratio (**FCR**) were calculated.

Body temperature measurement

Temperature sensors (Wuxi Fofia Technology Co., LTD., ET870, Jiangsu, China) were installed under the wings to continuously monitor the body temperature of broilers after *Escherichia coli* infection.

Sample collection

24 h after *Escherichia coli* infection, anticoagulant blood was collected from broilers wing veins using heparin sodium anticoagulant tube, and blood smears were prepared immediately. The blood samples were then centrifuged at 4 °C at 3000 × g for 10 min to prepare plasma, which was stored at −20 °C for subsequent analysis. Then the broilers were slaughtered, and the livers were collected and weighed to calculate the organ index. Organ index = organ weight (g)/body weight (g). Part of the liver tissues were placed in 4 % paraformaldehyde and the rest in

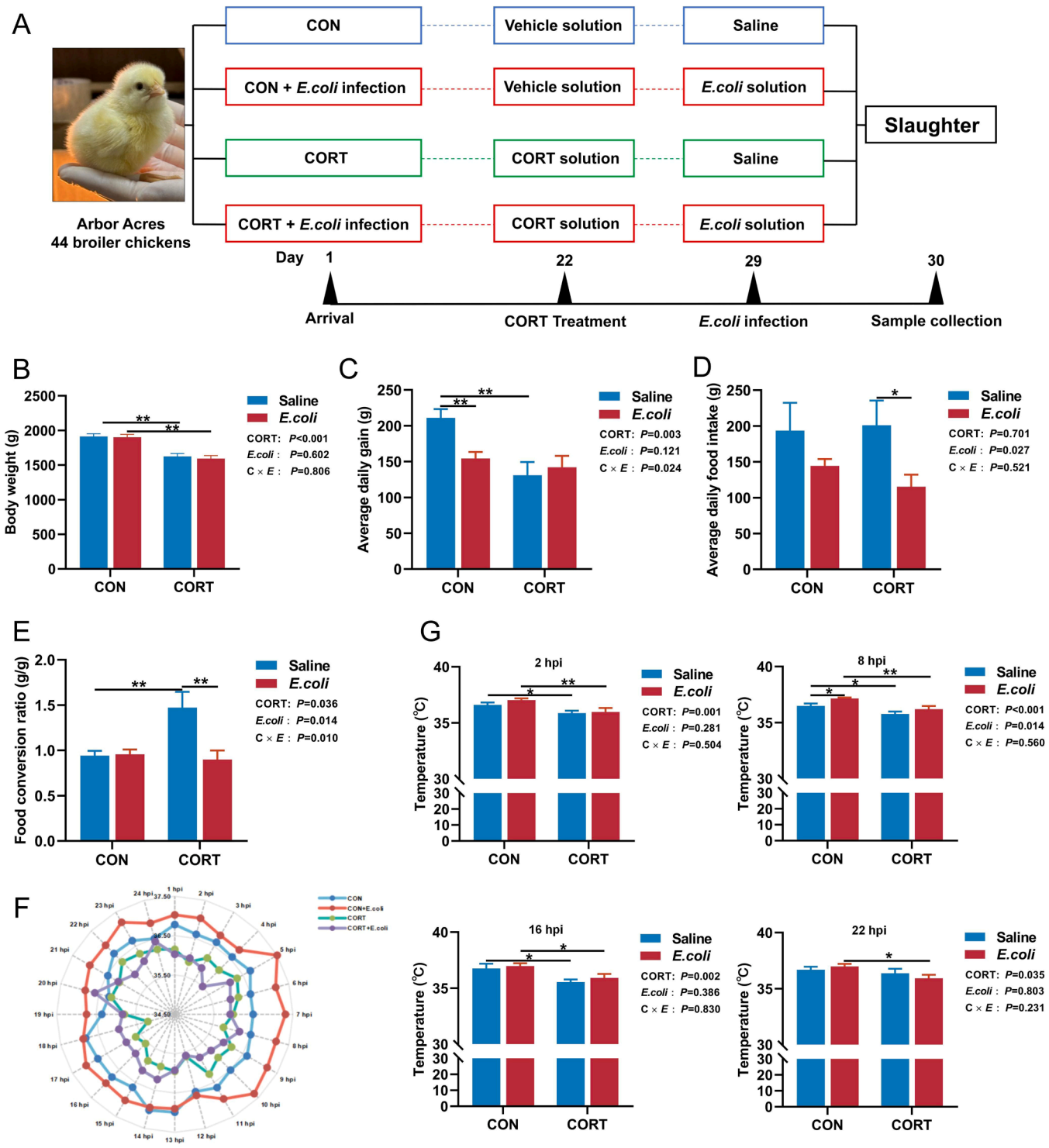

Fig. 1. Growth performance and body temperature of broilers treated with corticosterone or *E*scherichia coli or both. (A) Schematic diagram of the experimental design; (B) The BW of broilers at 30d; (C) The ADG of broilers at 30d; (D) The ADFI of broilers at 30d; (E) The FCR of broilers at 30d; (F) Continuous 24-hour monitoring of body temperature after corticosterone or *Escherichia coli* or both treatments. In the radar chart, different colored lines represent the continuous changes in body temperature of broilers in different groups, with the unit °C; (G) The body temperature of broilers at 2, 8, 16, and 22 h post corticosterone treatment or *Escherichia coli* infection or both. Data are presented as the mean ± SEM ($n = 9$ per group). The *P* values in the top right corner of each panel represent the results of two-way ANOVA. $P_{CORT} < 0.05$ indicates a significant effect of corticosterone treatment on the respective parameter. $P_{E.coli} < 0.05$ indicates a significant effect of *Escherichia coli* infection on the respective parameter. $P_{CORT \times E.coli} < 0.05$ indicates a significant interaction effect between corticosterone treatment and *Escherichia coli* infection on the respective parameter. $^*P < 0.05$, $^{**}P < 0.01$.

Table 1
Ingredients and nutrient composition of the diets for broilers.

Items	Day 1 to 21	Day 22 to 30
Ingredients, %		
Wheat	25.00	35.50
Corn powder	20.00	30.00
Corn meal	14.00	2.80
Soybean meal	12.00	4.00
Rice powder	10.00	8.00
Corn gluten powder	4.00	5.00
Feather powder	2.00	2.00
DDGS	2.00	0.00
Candy meal	1.00	4.00
Rapeseed meal	3.00	2.00
Corn	2.00	2.00
Soybean oil	0.50	0.70
Limestone	1.20	1.50
Calcium hydrogen phosphate	1.40	0.84
Sodium chloride	0.29	0.30
Lysine	0.81	0.64
Methionine	0.13	0.14
Tryptophan	0.01	0.02
Choline	0.10	0.06
Premix[1]	0.56	0.50
Calculated nutrient composition, %		
Metabolizable energy, kcal/kg	3100	3200
Crude protein	21.00	19.00
Calcium	1.30	1.20
Available phospholipid	0.60	0.50
Sodium chloride	0.80	0.80
Methionine	0.90	0.90

[1] The premix was composed of the following per kg diet: Vitamin A 9000 IU; Vitamin D3, 3600 IU; Vitamin E,12 IU; Vitamin K3, 3.00 mg; Vitamin B1, 2.00 mg; Vitamin B2, 6.90 mg; Vitamin B6, 2.70 mg; Vitamin B12, 0.02 mg; D-Biotin, 0.23 mg; Nicotinic acid, 31.20 mg; Folic acid, 1.00 mg; Vitamin B5, 10.80 mg; Choline chloride, 0.30 g; Fe (as FeSO4), 60.00 mg; Cu (as CuSO4), 12.00 mg; Mn, 90.00 mg; Zn (as ZnSO4), 90.00 mg; I (as KI), 0.80 mg; Se (as Na2SeO3), 0.30 mg.

liquid nitrogen, which were then transferred to −80 °C refrigerator for subsequent analysis.

Heterophil to lymphocyte (H/L) ratio

10 μL of fresh anticoagulant blood samples were collected from wing veins from each broiler and smeared on microscopic glass slides. The smears were air-dried and stained with Giemsa (BASO, WGO-020, Taipei, China). Then the smears were viewed with an optical microscope (Olympus-BX53, Tokyo, Japan) to count the number of leukocytes. A total of one hundred leukocytes were counted, including heterophil, lymphocyte, and monocytes. The H/L ratio was calculated as previous described (Thiam et al., 2022).

Plasma biochemical indices

The concentrations of aspartate aminotransferase (**AST**, H002), alanine aminotransferase (**ALT**, H001), lactate dehydrogenase (**LDH**, H008),total cholesterol (**T-CHO**, H202), triglyceride (**TG**, H201), total protein (**TP**, H102), and globulin (**GLOB**, H103) in plasma were determined by automatic biochemical analyzer (Hitachi, 7020, Tokyo, Japan), and the respective commercial assay kits were obtained from Meinkang Biotechnology Co., Ltd. (Ningbo, China). The concentration of albumin (**ALB**) in plasma was calculated by TP minus GLOB. All operations were performed in accordance with manufacturer's requirements.

Plasma corticosterone concentration

Corticosterone content in plasma was measured by using chicken Corticosterone ELISA Kit (Elabscience Biotechnology Co., Ltd., E-EL-0160, Wuhan, China) following the manufacturer's instructions. The plasma samples were diluted 25 times then measured. The detection limits of the kit is 0.39 to 25 ng/mL.

Inflammatory response indices

The concentrations of tumor necrosis factor-α (**TNF-α**, MM-0938O1, detection limits: 3 to 80 ng/L), interleukin-1β (**IL-1β**, MM-36910O1, detection limits: 3 to 120 ng/L), interleukin-10 (**IL-10**, MM-1145O1, detection limits: 1 to 48 ng/L), C-reactive protein (**CRP**, MM-0503O1, detection limits: 30 to 800 μg/L), complement 3 (**C3**, MM-1610O1, detection limits: 30 to 800 μg/mL), and lysozyme (**LZM**, MM-34261O1, detection limits: 0.03 to 2 μg/L) in plasma were determined by using chicken ELISA Kits (Jiangsu Meimian Industrial Co., Ltd., Yancheng, China). The plasma samples were diluted 5 times then measured. All operations were performed in accordance with manufacturer's requirements.

Hematoxylin and eosin (H&E) staining

The H&E staining was performed by Servicebio Technology Co., Ltd. (Wuhan, China). Briefly, the liver tissues ($n = 6$ per group) were fixed overnight in 4 % paraformaldehyde, and then dehydrated in a series of graded ethanol, embedded in paraffin wax, cut into 5-μm-thick sections, and stained with hematoxylin and eosin. The sections were scanned using a microscope slide scanner (Grundium Ocus, Finland) for further pathological analysis.

Oil red O staining

The Oil Red O staining was performed by Servicebio Technology Co., Ltd. (Wuhan, China). Briefly, the liver samples ($n = 3$ per group) were fixed in 4 % paraformaldehyde and sliced into 10-μm-thick sections, air-dried, rinsed with 60 % isopropanol, stained with Oil Red O solution for 15 min at 37 °C, and rinsed with 60 % isopropanol. The nucleus was counterstained with hematoxylin for 5 min. The sections were scanned using a microscope slide scanner (Grundium Ocus, Finland) for further analysis. Ten random felds (10 × magnifcation) were selected for each sample to measure the lipid droplet proportion as previous described (Cao et al., 2022). The measurements of lipid droplet proportion were conducted by using the Image J software (NIH, USA).

Immunohistochemical (IHC) staining

The IHC staining was performed by Servicebio Technology Co., Ltd. (Wuhan, China). Briefly, the liver tissue ($n = 6$ per group) was fixed with 4 % paraformaldehyde, dehydrated, embedded in paraffin, and deparaffinized. Then the sections were incubated with blocking medium and incubated with the primary antibodies at 4 °C overnight (**Caspase-3**, gb1109-1; **p62**, gb111998; **LC-3II**, gb11124, Servicebio Technology Co., Ltd., Wuhan, China). After washing in PBS, the sections were incubated with secondary antibodies with horseradish peroxidase. Subsequently, the sections were developed with chromogen substrate, and counterstained with hematoxylin. The staining results were visualized by using a microscope slide scanner (Grundium Ocus, Finland). Five random fields (40 × magnifcation) were selected for each section to measure the positive area proportion as previous described (Zhang et al., 2023), and quantified by Image J software (NIH, USA).

Total protein extraction and western blot

Total protein was extracted from an approximately 35 mg liver tissue as previously described (Duan et al., 2014). The protein concentration was determined by using the BCA protein assay kit obtained from Tsingke Biotech Co., Ltd. (DQ111-01, Nanjing, China). Then, the protein samples were subjected to 10 % SDS-PAGE gels for electrophoresis and transferred onto a nitrocellulose filter membrane. Western blot analysis

of phosphorylated-glucocorticoid receptor (**p-GR**, Cell Signaling Technology, Inc., 4161S, Massachusetts, USA) was conducted following the manufacturer's instruction. Tubulin-α (Bioworld Technology, Inc., BS1699, Minnesota, USA) was employed as the internal control. The membrane was incubated with Super-sensitive ECL chemiluminescent substrate (Labgic Technology Co., Ltd., BL520B, Beijing, China), and then the signals were captured using the VersaDoc 4000MP system (Bio-Rad, Hercules, CA). Image J software (NIH, USA) was applied to analyze the density of each band.

Liver RNA sequencing

The liver samples were entrusted to LC-Bio Technology Co., Ltd. (Hangzhou, China) for RNA sequencing. Briefly, the total RNA was extracted using Trizol regent (Thermofisher, 15596018, Waltham, USA) following the manufacturer's procedure and sequenced using the Illumina NovaSeq 6000 system for 2 × 150 bp paired-end sequencing (PE150). After the final transcriptome was generated, StringTie and ballgown were used to estimate the expression levels of all transcripts and perform expression abundance for mRNAs by calculating fragment per kilobase of transcript per million mapped reads (**FPKM**) value. The genes with the absolute fold change (**FC**) ≥ 2 and p value < 0.05 were defined as significantly differentially expressed genes (**DEGs**), and then subjected to enrichment analysis of Gene Ontology (**GO**) functions and Kyoto Encyclopedia of Genes and Genomes (**KEGG**) pathways. Omic-Studio tools (https://www.omicstudio.cn) were used for further analysis and making charts.

Chromatin immunoprecipitation sequencing (ChIP-Seq) analysis

TF-link database (https://tflink.net/browse/) was used for GR ChIP-Seq analysis. National Institutes of Health DAVID Bioinformatics (https://davidbioinformatics.nih.gov/) was applied to KEGG analysis. The online bioinformatics tool (http://bioinformatics.com.cn/) was utilized for result visualization.

Statistical analysis

All the data were presented as means ± SEM. The IBM SPSS 26.0 software (SPSS Inc., Chicago, IL, USA) was used for analyzed. Two-way ANOVA was performed to test the significance among different groups, following by the least squares difference (**LSD**) for post hoc comparison. The differences were considered statistically significant when $^{*}P < 0.05$ and $^{**}P < 0.01$.

Results

Growth performance and body temperature

Compared with CON group, BW and ADG of broilers in CORT group were significantly decreased ($P < 0.01$), while FCR was significantly increased ($P < 0.01$). *Escherichia coli* infection significantly decreased ADG ($P < 0.01$), and ADFI tended to decrease, but it had little effect on BW and FCR, compared with the CON group. In comparison to the CON + *E.coli* group, the BW of broilers in the CORT + *E.coli* group exhibited a significant reduction ($P < 0.01$), whereas no significant differences were observed in other measured parameters (Fig. 1B-E).

Additionally, the body temperature of broilers was continuously measured for 24 h after *Escherichia coli* infection, as shown in the radar chart (Fig. 1F). The temperature changes at different time points were statistically analyzed (Fig. 1G). The results showed that CORT treatment reduced the body temperature of broilers, while *Escherichia coli* infection increased the body temperature compared to CON group. However, compared with CON + *E.coli* group, the CORT + *E.coli* group had lower body temperature.

Stress indicators and biochemical indices

Compared with CON group, plasma corticosterone levels in CORT group ($P < 0.01$) and CON + *E.coli* group ($P < 0.05$) were significantly increased, while in CORT + *E.coli* group, the corticosterone content was significantly decreased ($P < 0.01$) compared with CON + *E.coli* group (Fig. 2A). Meanwhile, the blood smears were made to measure the H/L ratio (Fig. 2B). The statistical results showed that CORT treatment ($P < 0.01$) and *Escherichia coli* infection ($P < 0.05$), comparing with CON group, significantly increased H/L ratio. In comparison with CON + *E. coli* group, H/L ratio in CORT + *E.coli* group showed an increasing trend ($P = 0.05$) (Fig. 2C).

Biochemical detection results showed that compared with CON group, CORT treatment significantly increased the contents of AST, AST/ALT, LDH, T-CHO and TG in plasma ($P < 0.01$), and *Escherichia coli* infection significantly increased the plasma contents of AST and AST/ALT ($P < 0.01$). The plasma contents of ALT ($P < 0.01$), AST ($P < 0.01$) and LDH ($P < 0.05$) in CORT + *E.coli* group were significantly decreased, and T-CHO and TG levels were significantly increased ($P < 0.01$) compared with CON + *E.coli* group (Fig. 2D-I).

Immune response parameters

To further explore the effects of CORT treatment or *Escherichia coli* infection or both on immune response in broilers, we detected plasma concentrations of inflammatory cytokines and innate immune molecules. The results showed that, compared with CON group, CORT treatment significantly increased the plasma concentrations of IL-10, TP, ALB, and GLOB ($P < 0.01$), as well as LZM ($P < 0.05$), and tended to decrease the TNF-α concentration ($P = 0.06$). Compared with CON group, *Escherichia coli* infection significantly decreased the level of IL-10 ($P < 0.01$) in plasma, and increased the levels of LZM, TP, and GLOB ($P < 0.01$). In comparison with CON + *E.coli* group, the plasma concentration of IL-1β was significantly decreased ($P < 0.01$), while the concentrations of IL-10, TP, ALB, and GLOB were significantly increased ($P < 0.01$), and LZM tended to be increased ($P = 0.05$) in CORT + *E.coli* group (Fig. 3A-I).

Liver pathological damage

Necropsy. Compared with the CON group, CORT treatment significantly increased the liver weight and liver index of broilers ($P < 0.01$), leading to hepatomegaly and a yellowish-brown appearance. Compared with the CON + *E. coli* group, the liver volume of broilers in the CORT + *E. coli* group was reduced, and the liver weight was significantly decreased ($P < 0.05$) (Fig. 4A-C).

Oil Red O staining. CORT treatment significantly increased the proportion of lipid droplets in liver ($P < 0.01$), while *Escherichia coli* infection had a tendency to increase the lipid droplet proportion compared with CON group. Interestingly, compared with CORT group, lipid droplet proportion in CORT + *E.coli* group was significantly decreased ($P < 0.01$) (Fig. 4D and E).

H&E staining. Then we further observed the histopathological changes of the liver by H&E staining. The liver tissue of broilers in the CON group showed a normal structure, with hepatic cell cords arranged in a radial pattern and hepatocytes were intact. In contrast to the CON group, the liver tissue of broilers in the CORT group exhibited disrupted structural integrity, with the presence of vacuoles within hepatocytes and the occurrence of steatosis. *Escherichia coli* infection led to the loss of normal liver structure, hepatocyte rupture and disruption of integrity. Additionally, the liver tissue had congestion and significant inflammatory cell infiltration. However, compared with CON + *E.coli* group, hepatocytes in CORT + *E.coli* group had a certain degree of structural destruction and inflammatory cell infiltration, but the degree of lesion was less severe (Fig. 4F).

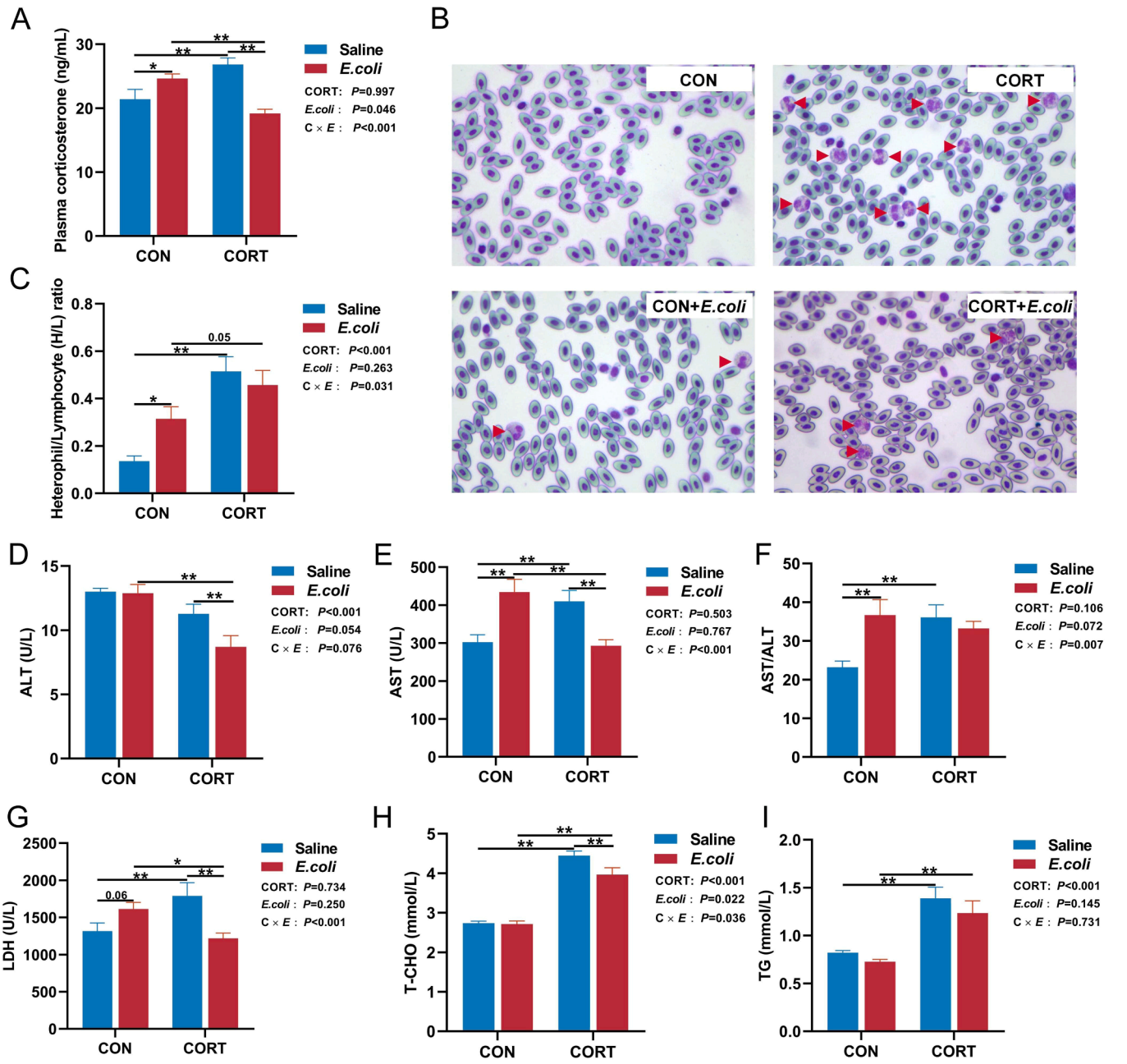

Fig. 2. The effects of corticosterone treatment or Escherichia coli infection or both on stress indices and biochemical parameters concentrations in plasma. (A) The corticosterone concentration in plasma; (B) The representative blood smears of each group. The red arrow represents heterophil; (C) The heterophil to lymphocyte (H/L) ratio; (D) ALT concentration in plasma; (E) AST concentration in plasma; (F) AST to ALT (AST/ALT) ratio; (G) LDH concentration in plasma; (H) T-CHO concentration in plasma; (I) TG concentration in plasma. Data are presented as the mean ± SEM ($n = 8$ per group). The P values in the top right corner of each panel represent the results of two-way ANOVA. $P_{CORT} < 0.05$ indicates a significant effect of corticosterone treatment on the respective parameter. $P_{E.coli} < 0.05$ indicates a significant effect of Escherichia coli infection on the respective parameter. $P_{CORT \times E.coli} < 0.05$ indicates a significant interaction effect between corticosterone treatment and *Escherichia coli* infection on the respective parameter. $^{*}P < 0.05$, $^{**}P < 0.01$.

RNA sequencing analysis

DEGs. To further investigate the underlying mechanisms of different responses in broiler liver under CORT exposure or *Escherichia coli* infection or both, we performed transcriptome sequencing of liver tissues. Supplementary Fig. 1 showed the volcano maps and heat maps of DEGs in each comparison group. Compared with CON group, 437 genes were significantly up-regulated and 331 genes were significantly down-regulated in CORT group (Supplementary Fig. 1A and D). In CON + *E. coli* group, 251 genes were significantly up-regulated and 104 genes were significantly down-regulated compared with CON group (Supplementary Fig. 1B and E). In addition, 119 genes were significantly up-regulated and 448 genes were significantly down-regulated in CORT + *E.coli* group, compared with CON + *E.coli* group (Supplementary Fig. 1C and F). The Venn diagram showed the overlap of DEGs in different comparison groups (Supplementary Fig. 1 G).

GO term and KEGG pathway enrichment analysis. GO term enrichment analysis was used to understand the different functions associated with DEGs in different comparison groups, which were classified into three main domains: biological process, cellular component and molecular function. KEGG pathway enrichment analysis was performed to further identify the biological pathways significantly

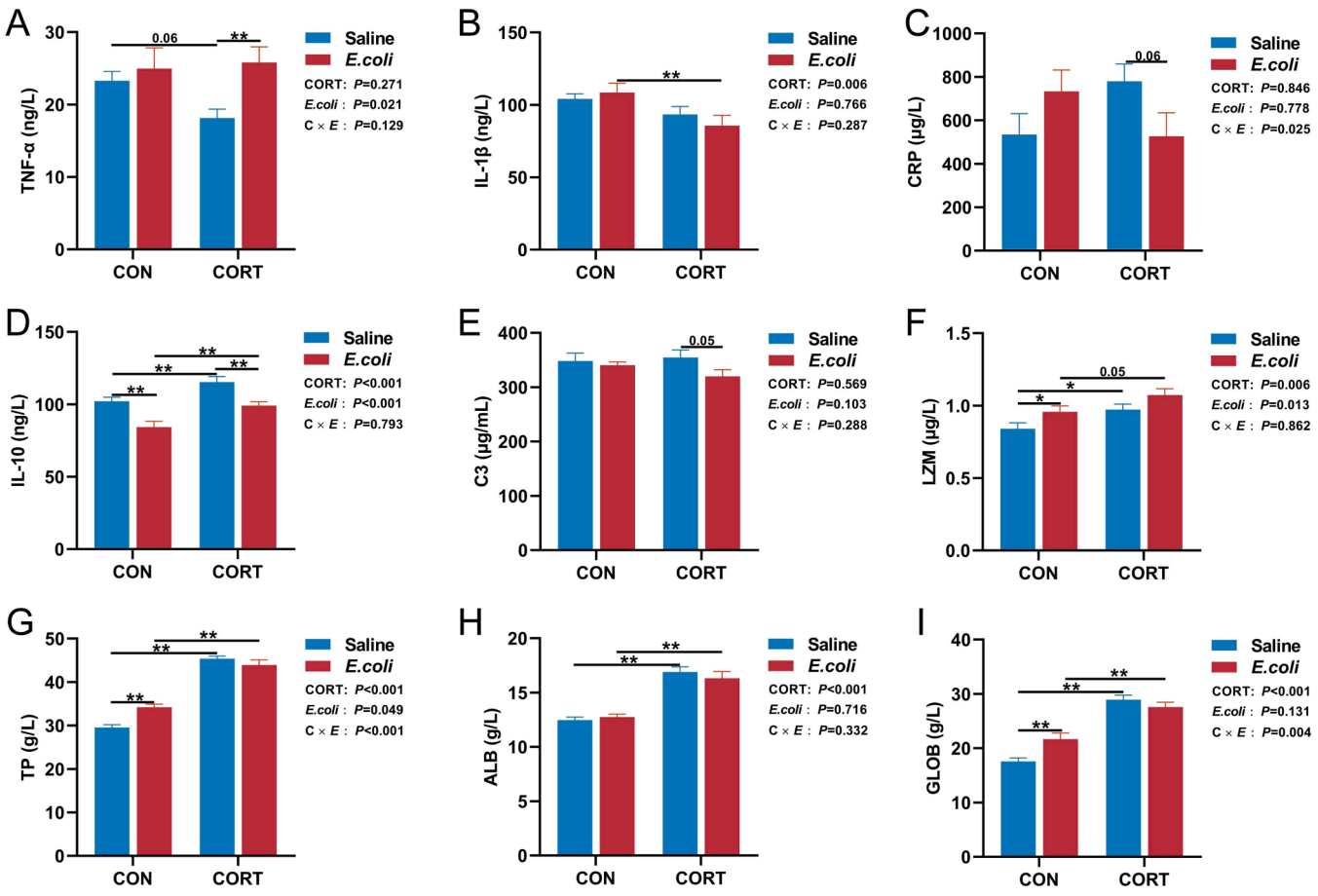

Fig. 3. The effects of corticosterone treatment or Escherichia coli infection or both on plasma inflammatory markers. (A) TNF-α concentration in plasma; (B) IL-1β concentration in plasma; (C) CRP concentration in plasma; (D) IL-10 concentration in plasma; (E) C3 concentration in plasma; (F) LZM concentration in plasma; (G) TP concentration in plasma; (H) ALB concentration in plasma; (I) GLOB concentration in plasma. Data are presented as the mean ± SEM ($n = 8$ per group). The P values in the top right corner of each panel represent the results of two-way ANOVA. $P_{CORT} < 0.05$ indicates a significant effect of corticosterone treatment on the respective parameter. $P_{E.coli} < 0.05$ indicates a significant effect of *Escherichia coli* infection on the respective parameter. $P_{CORT \times E.coli} < 0.05$ indicates a significant interaction effect between corticosterone treatment and *Escherichia coli* infection on the respective parameter. $^{*}P < 0.05$, $^{**}P < 0.01$.

associated with the DEGs.

CORT group v.s. CON group. The differences in biological process, cellular component and molecular function between CON group and CORT group were obtained by analyzing the 768 DEGs. Fig. 5A showed the top 12, 10, and 10 significantly enriched terms in biological process, cellular component, and molecular function, respectively. In biological process, positive regulation of cytokinesis and defense response were significantly enriched, and in molecular function, CCR6 chemokine receptor binding and chemokine activity were significantly enriched. Top 20 significantly enriched pathways by KEGG analysis were shown in Fig. 5B, including metabolic pathways, cytokine-cytokine receptor interaction, alanine, aspartate and glutamate metabolism, PPAR signaling pathway, glutathione metabolism, biosynthesis of amino acids and so on. In addition, we observed that among all the differentially expressed pathways, most were enriched into amino acid metabolism and lipid metabolism. Part of the DEGs and their enriched pathways were shown in Fig. 5C. Then we focused on the effects of CORT treatment on immune-related pathways and lipid metabolism pathways. In cytokine-cytokine receptor interaction pathway, the expression of *IL1R2, CSF3R, IL21R, IL1RL1, CCL4*, and *IL8L2* genes was significantly up-regulated, indicating that CORT treatment affected the immune function of liver. In terms of lipid metabolism, the expression of *FABP1, FABP4, PLIN1*, and *MMP1* genes in PPAR signaling pathway was significantly up-regulated, while the expression of *LPL* and *RXRG* genes was significantly down-regulated after CORT treatment, indicating that CORT treatment significantly affected liver lipid metabolism (Fig. 5D).

CON + E.coli group v.s. CON group. The differences in biological process, cellular component and molecular function between CON group and CON + *E.coli* group were obtained by analyzing the 355 DEGs. As shown in Fig. 6A, top 12, 10, and 10 significantly enriched terms in biological process, cellular component, and molecular function, respectively. In biological process, regulation of immune system process and glucocorticoid biosynthetic process, and in molecular function, protein-glutamine gamma-glutamyltransferase activity and glutathione binding were significantly enriched. Top 20 significantly enriched pathways by KEGG analysis were shown in Fig. 6B. After *Escherichia coli* infection, the classical pathways related to immune response, such as cytokine-cytokine receptor interaction, Toll-like receptor signaling pathway, MAPK signaling pathway and arachidonic acid metabolism pathway, were significantly enriched, indicating that *Escherichia coli* infection caused liver immune response in broilers. Furthermore, the PPAR signaling pathway and the steroid hormone biosynthesis pathway were also significantly enriched, suggesting their potential roles in the process of *Escherichia coli* infection in broilers. Part of the DEGs and their enriched pathways were shown in Fig. 6C. In the immune-related pathways, the expression of *CSF3, CSF3R, IL1R2, TLR1A* and *MAP3K8* genes was significantly up-regulated. In addition, the expression of *ACKR2, FABP3, MMP1, CYP11A1*, and *CYP21A1* genes in lipid metabolism and steroid hormone biosynthesis pathway was significantly up-regulated after *Escherichia coli* infection (Fig. 6D).

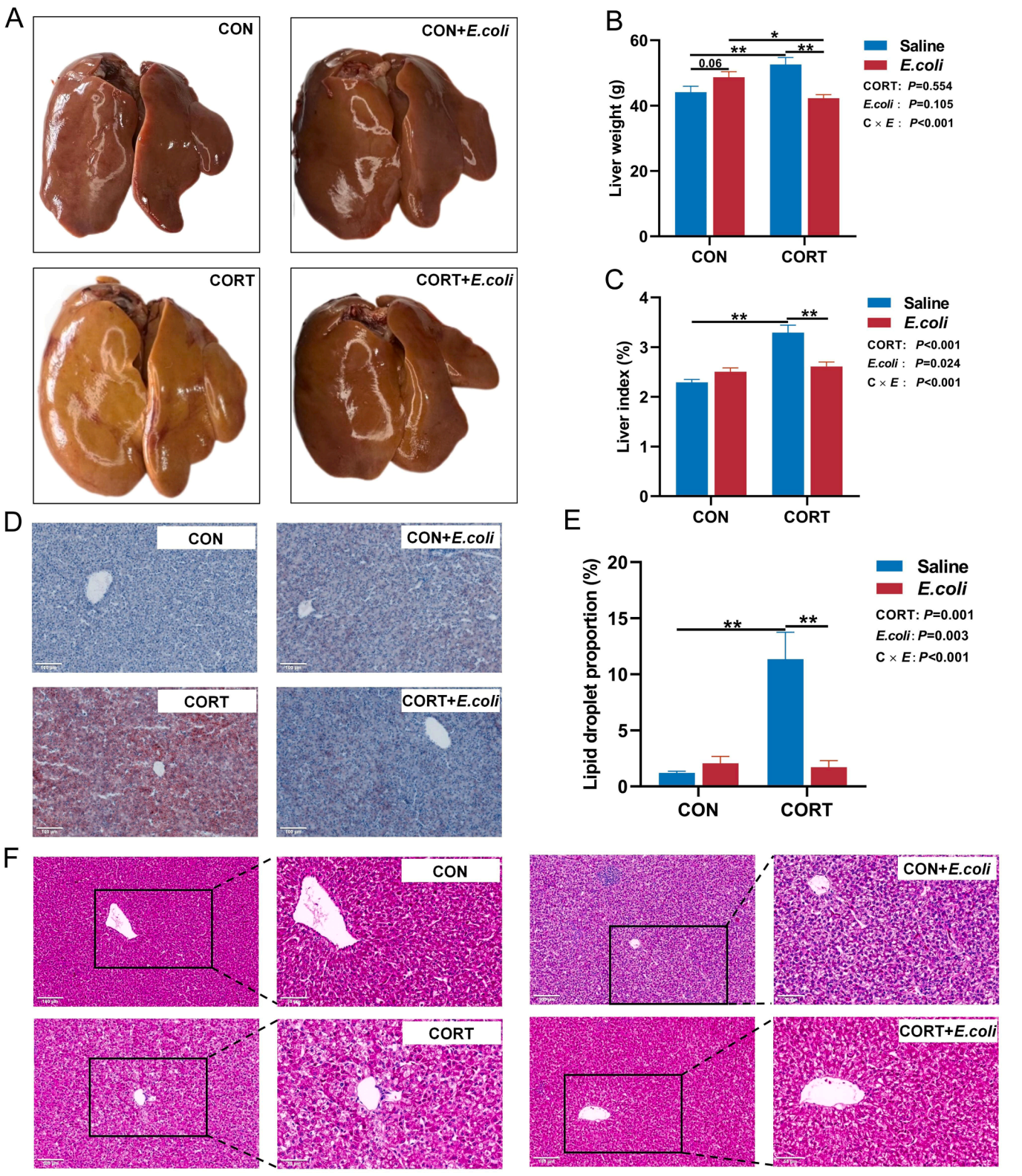

Fig. 4. Liver histopathological changes and lipid deposition in broilers treated with corticosterone or Escherichia coli infection or both. (A) Representative images of liver morphology; (B) The weight of liver; (C) The liver index ($n = 9$ per group). Liver index = liver weight (g)/body weight (g); (D) Representative images of liver Oil Red O staining ($n = 3$ per group). Magnification = 10 ×, scale bar = 100 μm; (E) Statistics of lipid droplet proportion; (F) Representative images of liver H&E staining ($n = 6$ per group). Magnification = 10 × (left) and 20 × (right), scale bar = 100 μm and 50 μm, respectively. Data are presented as the mean ± SEM. The *P* values in the top right corner of each panel represent the results of two-way ANOVA. $P_{CORT} < 0.05$ indicates a significant effect of corticosterrone treatment on the respective parameter. $P_{E.coli} < 0.05$ indicates a significant effect of *Escherichia coli* infection on the respective parameter. $P_{CORT \times E.coli} < 0.05$ indicates a significant interaction effect between corticosterone treatment and *Escherichia coli* infection on the respective parameter. $^{*}P < 0.05$, $^{**}P < 0.01$.

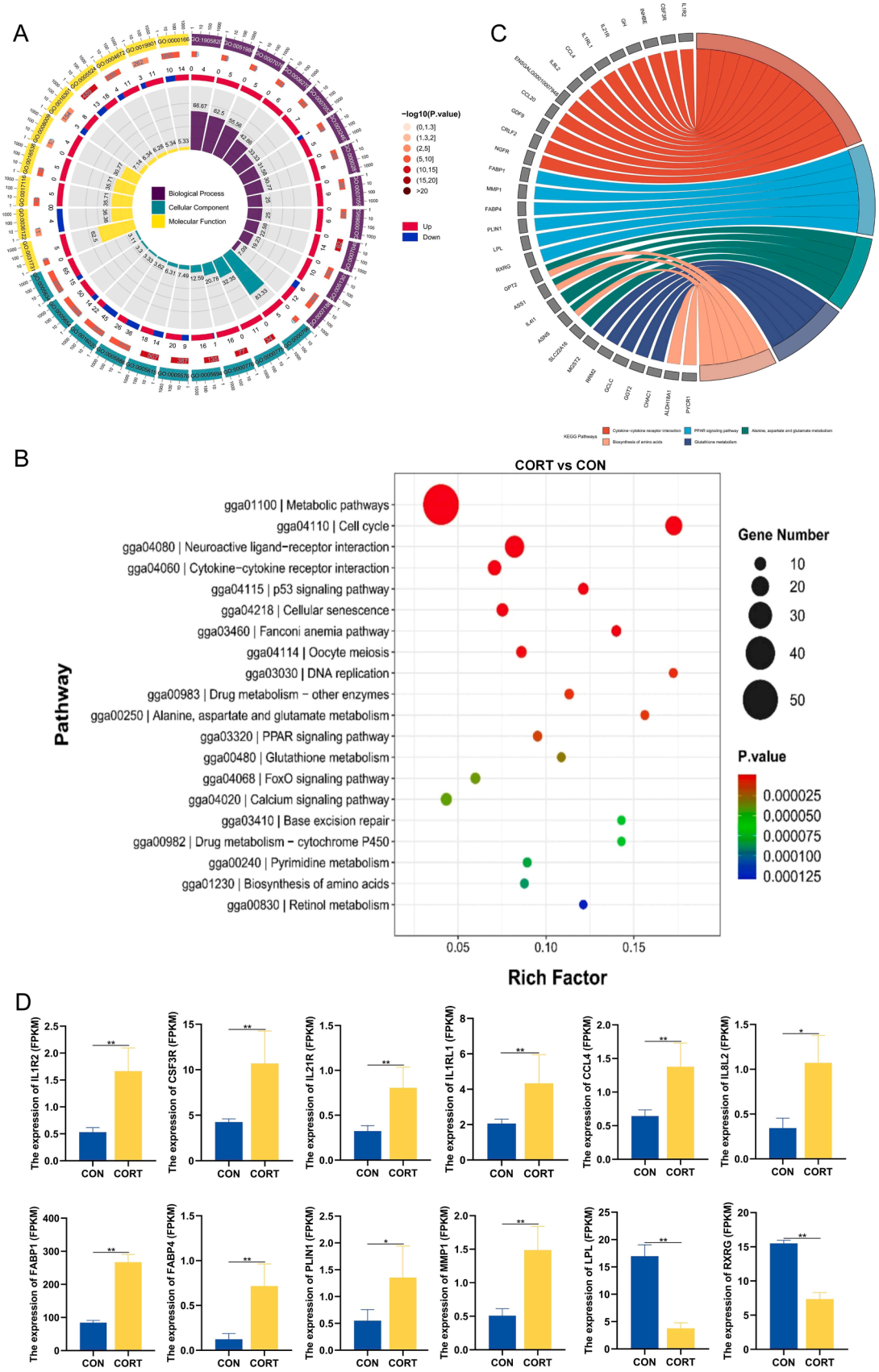

Fig. 5. GO and KEGG enrichment analysis of DEGs in broilers liver between CON group and CORT group. (A) GO enrichment analysis of DEGs between CON group and CORT group; (B) KEGG enrichment analysis of DEGs between CON group and CORT group; (C) Chord diagram of differentially expressed pathways and their corresponding genes between CON group and CORT group; (D) Bar chart of DEGs (n = 6 per group).

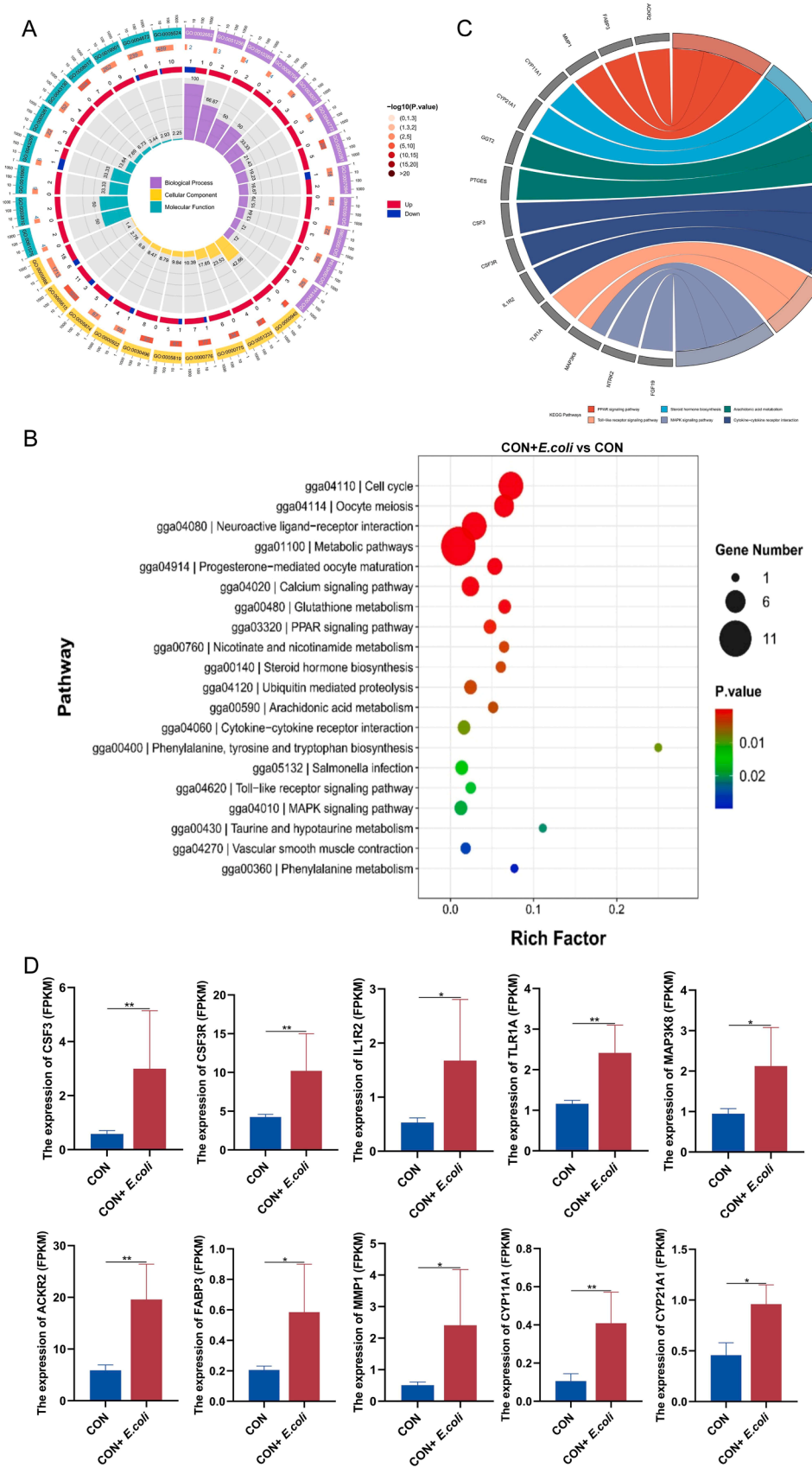

Fig. 6. GO and KEGG enrichment analysis of DEGs in broilers liver between CON group and CON + *E.*coli group. (A) GO enrichment analysis of DEGs between CON group and CON + *E.coli* group; (B) KEGG enrichment analysis of DEGs between CON group and CON + *E.coli* group; (C) Chord diagram of differentially expressed pathways and their corresponding genes between CON group and CON + *E.coli* group; (D) Bar chart of DEGs ($n = 6$ per group).

CORT + E.coli group v.s. CON + E.coli group. A total of 567 DEGs in CON + *E.coli* group and CORT + *E.coli* group were used for further analysis. Fig. 7A showed the top 12, 10, and 10 significantly enriched terms in biological process, cellular component, and molecular function, respectively. In biological process, response to redox state, vacuolar acidification and L-arginine transmembrane transport, and in molecular function, L-arginine transmembrane transporter activity and phosphatidylinositol 3-kinase binding were significantly enriched. Fig. 7B showed the top 20 significantly enriched pathways by KEGG analysis, including cytokine-cytokine receptor interaction, PPAR signaling pathway, steroid hormone biosynthesis, arachidonic acid metabolism, MAPK signaling pathway, p53 signaling pathway. Additionally, among all differentially expressed pathways, we noted a significant enrichment in the phagosome pathway. Fig. 7C showed a subset of these pathways and their associated DEGs. Compared with CON + *E.coli* group, the expression of *EDA2R, TNFRSF10B, TNFRSF6B* and *TNFRSF13B* genes in CORT + *E.coli* group was significantly down-regulated in cytokine-cytokine interaction pathway. The MAPK signaling pathway was also significantly down-regulated in CORT + *E.coli* group, as evidenced by a marked decrease in the expression of *JUN* and *JUND,* compared with CON + *E.coli* group. In terms of lipid metabolism, PPAR signaling pathway, steroid hormone synthesis and arachidonic acid metabolism pathway were significantly enriched, with significantly up-regulated gene expression of *PCK1, CYP3A5* and *CYP2C18*, and significantly down-regulated gene expression of *ACKR2, PLIN1* and *MMP1* in CORT + *E.coli* group. In addition, we also observed that the expression of *ATP6V0D2* gene was significantly up-regulated in the phagosome pathway, which was involved in vacuolar acidification in GO analysis (Fig. 7D).

Immunohistochemical staining of apoptosis and autophagy proteins

In liver RNA-Seq analysis, we observed significant changes in pathways associated with apoptosis, such as the p53 signaling pathway, as well as moderate changes in the autophagy pathway. To further elucidate these findings, we utilized IHC staining to assess the protein levels associated with apoptosis and autophagy in broiler liver under CORT treatment or *Escherichia coli* infection or both. CORT treatment had little effect on Caspase-3 protein expression, and *Escherichia coli* infection significantly increased the level of Caspase-3 protein ($P < 0.05$), indicating that *Escherichia coli* infection induced apoptosis in liver tissues. Compared with CON + *E.coli* group, the Caspase-3 protein expression of liver in CORT + *E.coli* group was significantly decreased ($P < 0.05$), suggesting that the degree of apoptosis was decreased (Fig. 8A and B). In comparison to CON group, CORT treatment had no significant effect on p62 protein expression, but significantly decreased the protein expression of LC-3II ($P < 0.05$). *Escherichia coli* infection significantly increased the protein expression of p62 ($P < 0.05$) and decreased the level of LC-3II ($P < 0.05$), suggesting that *Escherichia coli* infection inhibited liver autophagy. The protein expression of p62 was significantly decreased ($P < 0.01$), and LC-3II tended to increased in CORT + *E.coli* group, compared with CON + *E.coli* group, suggesting that the autophagy level in broiler liver was increased (Fig. 8C-F).

Western blot and ChIP-Seq analysis

Glucocorticoid binds to GR in cytoplasm to exert their biological effects, while p-GR regulates gene transcription by binding to the promoter regions of target genes. The expression of p-GR protein in liver tissues was detected by western blot. The results showed that compared with CON group, CORT treatment ($P < 0.01$) and *Escherichia coli* infection ($P < 0.05$) significantly increased p-GR protein expression in liver of broilers. However, compared with CON + *E.coli* group, the p-GR protein expression was significantly decreased in CORT + *E.coli* group ($P < 0.05$) (Fig. 9A). To investigate the regulatory relationship between GR and DEGs identified in liver RNA-Seq, we performed further analysis of GR ChIP-Seq and liver RNA-Seq data. The target genes regulated by GR were predicted by ChIP-Seq, followed by KEGG pathway analysis. The results were then compared with the KEGG analysis of liver RNA-Seq data. The overlapping pathways between the two analysis results included metabolic pathways, MAPK signaling pathway, PPAR signaling pathway, p53 signaling pathway, apoptosis, phagosome, cytokine-cytokine receptor interaction, Toll-like receptor signaling pathway and so on (Fig. 9B), suggesting that GR may be involved in regulating the biological processes of these pathways. Subsequently, we compared the predicted GR target genes with the DEGs identified in liver RNA-Seq for part of the pathways. The overlapping genes included *EDA2R, TNFRSF10B, PTGDS, FABP4, ATP6V0D2* and so on, suggesting that these genes may serve as downstream targets of GR (Fig. 9C).

Discussion

Avian pathogenic *Escherichia coli* (**APEC**) is a Gram-negative pathogen that widely infects poultry of various breeds and ages, causing significant adverse effects on growth performance and health condition, which results in considerable economic losses to the global poultry industry (Tan et al., 2024a). Furthermore, APEC has the potential for cross-species transmission and poses a significant threat to human health as a zoonotic pathogen (Bélanger et al., 2011). In the process of poultry breeding, various external factors, including temperature, humidity, feed quality, noise, and transportation, can place poultry in a state of stress, which will further weaken their production performance, and seriously affect the economic efficiency of farming (Ruan et al., 2023; Hu et al., 2024; Zhu et al., 2024). In this study, we investigated the effects of stress, *Escherichia coli* infection and their superposition on broilers growth performance, immune response and liver function, in order to provide theoretical basis for poultry health management and disease prevention.

APEC infection and stress have significant negative effects on poultry production performance. Previous studies have shown that APEC infection in broilers significantly reduces BW, ADG and ADFI, and FCR increases significantly (Tan et al., 2024b; Mao et al., 2024). Chronic heat stress has also been confirmed to significantly suppress the growth rates of broiler (Mohammed et al., 2019; Liu et al., 2023). Consistent with these findings, in the present study, we observed a significant reduction in ADG following APEC infection, and CORT treatment significantly decreased BW and ADG and increased FCR. However, compared to APEC infection alone, broilers pretreated with CORT followed by APEC infection exhibited a significantly lower BW, despite no notable effects on other parameters. Therefore, we speculated that certain biological processes within broilers may undergo significant alterations under these conditions.

Body temperature is an important and direct indicator of physiological state of an organism. When the body is affected by pathogens, an increase in body temperature helps to facilitate pathogen clearance. Studies have shown that the body temperature of laying hens increased significantly after infection with *Escherichia coli* (O157:H7) (Mehaisen et al., 2016). In the present study, consistent with previous reports, we found that the body temperature of broilers was consistently higher than that of the control group after APEC infection, with a significant increase starting at 5 h post infection. In addition, heat stress has been shown to increase rectal temperature in broilers (Mohammed et al., 2019; Luo et al., 2022). However, there are few studies on the effect of CORT treatment on broiler body temperature. Our results indicated that CORT treatment significantly reduced body temperature of broilers. Furthermore, the body temperature of broilers infected with APEC after CORT pretreatment was significantly lower than that of those infected with APEC alone. It is reasonable to speculate that it may be caused by a low basal body temperature induced by CORT treatment.

APEC infection can induce inflammatory responses in poultry. Meng et al. found that APEC infection increased the levels of TNF-α, IL-1β and IL-6 in chicken serum (Meng et al., 2024), and decreased the level of

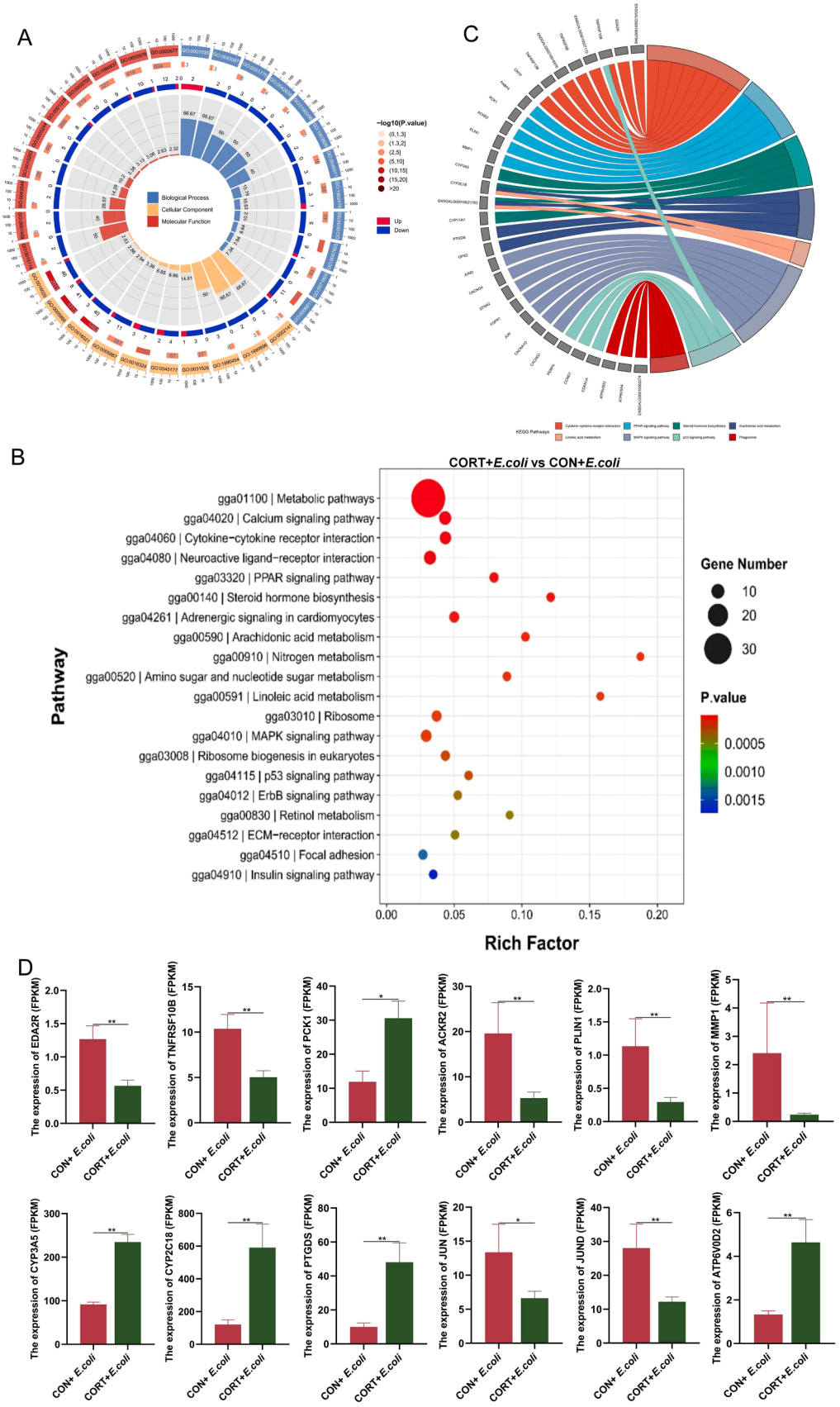

Fig. 7. GO and KEGG enrichment analysis of DEGs in broilers liver between CON + *E.*coli group and CORT + *E.*coli group. (A) GO enrichment analysis of DEGs between CON + *E.*coli group and CORT + *E.*coli group; (B) KEGG enrichment analysis of DEGs between CON + *E.*coli group and CORT + *E.*coli group; (C) Chord diagram of differentially expressed pathways and their corresponding genes between CON + *E.*coli group and CORT + *E.*coli group; (D) Bar chart of DEGs ($n = 6$ per group).

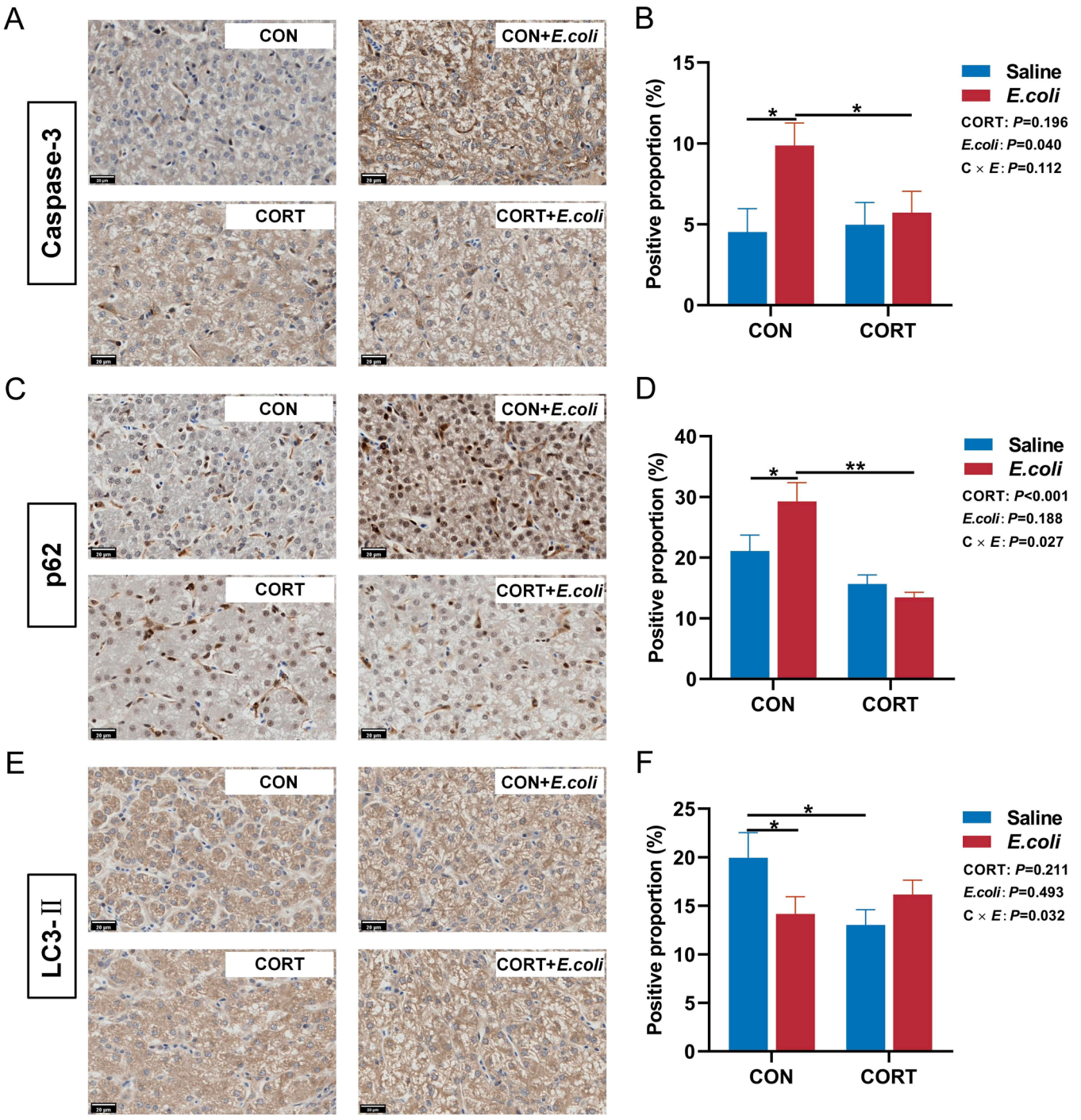

Fig. 8. Immunohistochemical (IHC) staining of broilers liver treated with corticosterone or *Escherichia coli* infection or both. (A) Representative images of Caspase-3 IHC staining; (B) Statistics of Caspase-3 positive proportion; (C) Representative images of p62 IHC staining; (D) Statistics of p62 positive proportion; (C) Representative images of LC-3II IHC staining; (D) Statistics of LC-3II positive proportion. Data are presented as the mean ± SEM ($n = 6$ per group). Magnification = 40 ×, scale bar = 20 μm. The *P* values in the top right corner of each panel represent the results of two-way ANOVA. $P_{CORT} < 0.05$ indicates a significant effect of corticosterone treatment on the respective parameter. $P_{E.coli} < 0.05$ indicates a significant effect of *Escherichia coli* infection on the respective parameter. $P_{CORT \times E.coli} < 0.05$ indicates a significant interaction effect between corticosterone treatment and *Escherichia coli* infection on the respective parameter. $^{*}P < 0.05$, $^{**}P < 0.01$.

IL-10 (Tan et al., 2024b). Consistent with these findings, our study demonstrated a significant reduction in plasma IL-10 level in broilers following APEC infection. In addition to affecting production performance, stress also impacts immune function, with the extent of the effects varying depending on the type, intensity, duration of stress, and species involved. For example, 21 days of continuous heat stress led to an inflammatory response in Arbor Acres broilers, characterized by significantly increased plasma levels of TNF-α and IL-1β, and a marked decrease in IL-10 levels (Li et al., 2023). In contrast, Dai et al. found that DEX treatment in White Leghorns resulted in immunosuppression, with significant reductions in plasma levels of IL-6 and IL-1β (Dai et al., 2022). In the present study, CORT treatment decreased plasma TNF-α level and significantly increased IL-10 level in broilers. Notably, the innate immune molecules levels in plasma, including LZM, TP, ALB and GLOB, were significantly elevated after CORT treatment, indicating that the regulation of the immune system by CORT was both complex and

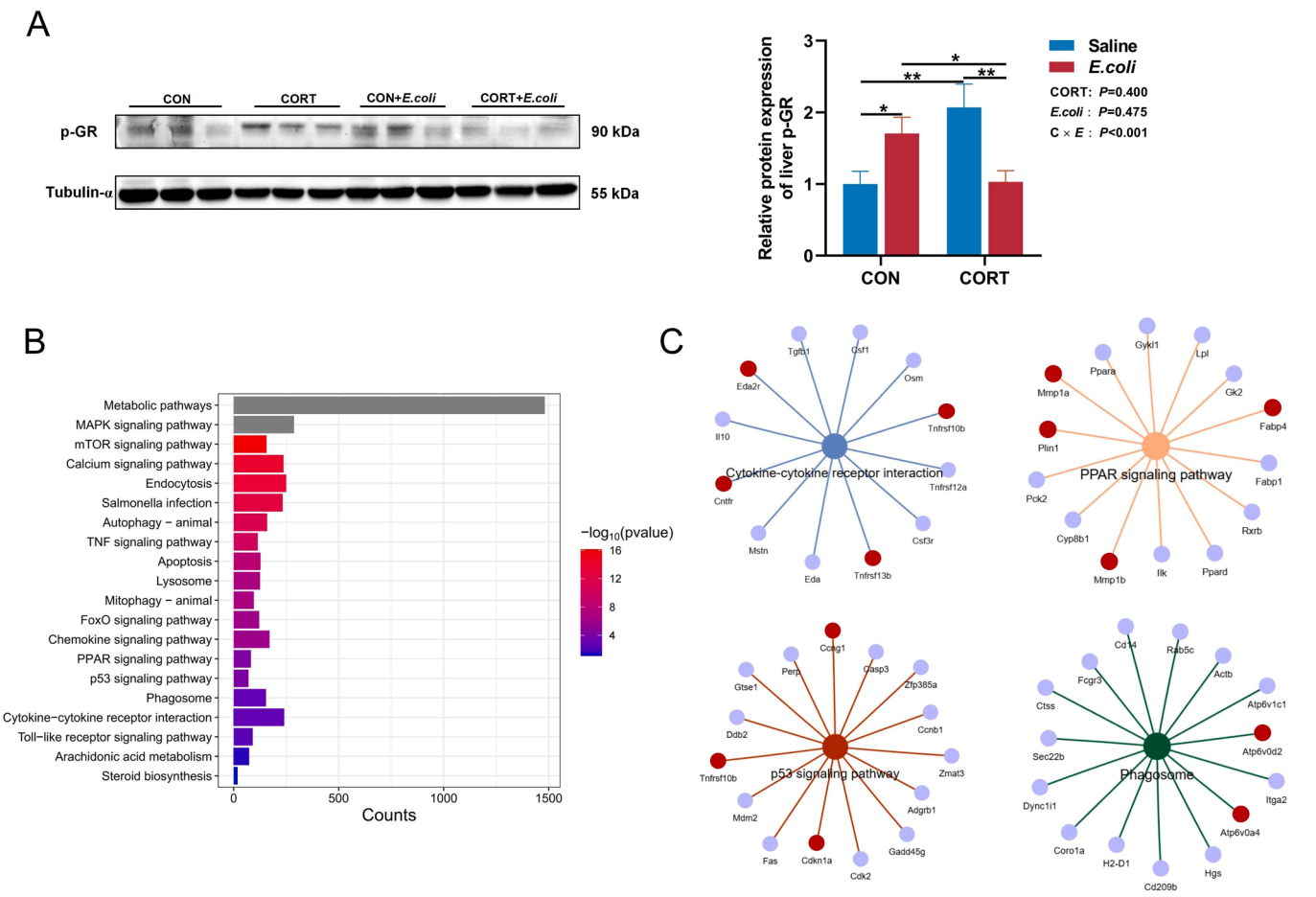

Fig. 9. Western blot analysis of p-GR and GR ChIP-Seq analysis of broilers liver treated with corticosterone or Escherichia coli infection or both. (A) Representative bands and the quantified statistic of p-GR in western blot. Protein expression was normalized to the respective abundance of Tubulin-α; (B) KEGG analysis of the target genes of GR predicted by ChIP-Seq; (C) Overlapping of GR predicted target genes and DEGs identified by RNA-Seq. The red circles represented overlap genes. Data are presented as the mean ± SEM ($n = 8$ per group). The P values in the top right corner of each panel represent the results of two-way ANOVA. $P_{CORT} < 0.05$ indicates a significant effect of corticosterone treatment on the respective parameter. $P_{E.coli} < 0.05$ indicates a significant effect of *Escherichia coli* infection on the respective parameter. $P_{CORT \times E.coli} < 0.05$ indicates a significant interaction effect between corticosterone treatment and *Escherichia coli* infection on the respective parameter. $^{*}P < 0.05$, $^{**}P < 0.01$.

dynamic. Specifically, CORT treatment may compensatory enhancing the innate immunity to maintain immune balance of broilers. Currently, research on how animals respond to pathogen infections under stress status is relatively limited. Previous studies have shown that chronic heat stress induced an intestinal inflammatory response, and the combination of chronic heat stress with *Salmonella Enteritidis* infection exacerbated the severity of enteritis, disrupted the intestinal barrier, and ultimately facilitated the translocation of pathogens from the intestine to the spleen of broilers (Quinteiro-Filho et al., 2012; Tang et al., 2021). However, Bailey et, al. found that repeated social defeat increased the number of splenic macrophages and the expression of TLRs on these macrophages in mice, which ultimately resulting in an enhanced bactericidal activity (Bailey et al., 2007). In the present study, compared to APEC infection alone, CORT pretreatment followed by APEC infection significantly reduced plasma IL-1β level, while markedly increased the levels of IL-10, LZM, TP, ALB and GLOB in broilers, indicating a stronger innate immune response in broilers with CORT pretreatment. In the present study, although CORT treatment enhanced the innate immunity of broilers to some extent, it also had a negative impact on their growth performance. In poultry farming, whether the trade-off between enhanced immunity and reduced growth performance is economically viable and feasible remains to be further evaluated. Additionally, it is necessary to explore potential strategies that can minimize the negative effects while maintaining the enhanced immune response.

Perihepatitis is a characteristic symptom observed in poultry after APEC infection, resulting in liver damage (Hu et al., 2022; Meng et al., 2024). In this study, APEC infection led to hepatomegaly in broilers, accompanied by a significant increase in plasma levels of AST, ASL/ALT and LDH. Additionally, H&E staining revealed disrupted hepatic architecture, ruptured hepatocytes, and extensive infiltration of inflammatory cells within the liver tissue, indicating that APEC infection induced inflammatory response and liver damage, consistent with previous research (El-Shenawy et al., 2023; Meng et al., 2024). Moreover, studies have shown that stress can also cause liver damage in poultry. Cruvinel et al. reported that cyclical heat stress resulted in significantly higher serum AST and ALT levels in broilers (Cruvinel et al., 2023). Consistent with these findings, our results demonstrated that CORT treatment significantly elevated plasma levels of AST, ASL/ALT and LDH in broilers, accompanied by the appearance of numerous vacuoles in liver cells, suggesting that CORT treatment induced liver damage in broilers. Furthermore, we observed that plasma levels of ALT, AST and LDH of broilers infected with APEC after CORT pretreatment were significantly reduced compared with that of APEC infection alone. H&E staining revealed a certain extent of liver damage, but the severity of the damage was less pronounced than that observed with APEC infection alone, suggesting that the liver damage was alleviated.

To further investigate the potential mechanisms underlying the effects of APEC infection or CORT treatment or both on broilers liver,

transcriptome sequencing was performed on liver tissue. A total of 335 DEGs were identified following APEC infection. The expression levels of *CSF3, CSF3R, IL1R2, TLR1A*, and *MAP3K8* were significantly up-regulated and were enriched in the cytokine-cytokine receptor interaction pathway, Toll-like receptor signaling pathway, and MAPK signaling pathway, suggesting that APEC infection triggered immune response to facilitate pathogen clearance and induced an inflammatory response in the liver (Zhang et al., 2018; Nihashi et al., 2019). In addition, we observed significant enrichment in lipid metabolism pathways, such as PPAR signaling pathway, arachidonic acid metabolism pathway and steroid hormone synthesis pathway. Previous research has shown that in the livers of *Escherichia coli* infected mice, lipid deposition occurred by promoting fatty acid uptake and triglyceride synthesis (Li et al., 2018). In the present study, although APEC infection had no significant effect on the content of T-CHO and TG in broiler plasma, the proportion of lipid droplet in liver tissue showed a tendency to increase, indicating that APEC infection changed liver lipid metabolism. These results indicate that APEC infection induce inflammatory response and tissue damage in the liver of broilers, while also affecting lipid metabolism.

Liver RNA-seq results showed that a total of 768 DEGs were identified after CORT treatment compared with CON group. Avian β-defensins (**AvBDs**) play a crucial role in the innate immunity of poultry, exhibiting broad-spectrum antimicrobial activity and serving as key substances for avian defense against exogenous pathogens. Due to the lack of effective oxidative mechanisms in avian heterophils, poultry may rely more on antimicrobial peptides such as AvBDs to resist infections (Zhang and Sunkara, 2014). In this study, the expression levels of *AvBD9, AvBD10, AvBD13*, and *AvBD14* were significantly up-regulated following CORT treatment, suggesting an enhancement of the innate immune function in broilers. In the cytokine-cytokine receptor interaction pathway, gene expression levels of *IL1R2, CSF3R, IL21R, IL1RL1, CCL4*, and *IL8L2* were significantly up-regulated. The up-regulation of these genes suggested that the liver immune response was comprehensively activated under stress. Furthermore, *CSF3R* and *IL21R* also play roles in cell proliferation and differentiation, and the aggregation of immune cells may contribute to liver repair processes induced by stress (Korbecki et al., 2020). In the PPAR signaling pathway, the expression of *FABP1, FABP4, PLIN1*, and *MMP1* genes was significantly up-regulated, indicating enhanced hepatic lipid droplets formation and lipid storage capacity (Su et al., 2024). These changes implied that CORT treatment induced liver lipid metabolism reprogramming and ultimately led to liver lipid deposition, which was consistent with our previous work (Liu et al., 2024). The above results indicate that CORT treatment affect the immune function, while reprogramming the lipid metabolism in liver of broilers.

In the transcriptomic analysis of APEC infection alone and APEC infection with CORT pretreatment comparison groups, a total of 567 DEGs were identified. The expression levels of *EDA2R* and *TNFRSF10B* were significantly down-regulated, which play a crucial role in the regulation of apoptosis (Guan et al., 2024). To validate these findings, we assessed the expression of the apoptosis marker protein Caspase-3 in liver tissue. The results demonstrated that APEC infection after CORT pretreatment significantly reduced the expression of Caspase-3 in liver compared with APEC infection alone, indicating that the hepatic apoptosis was inhibited. In addition, we observed that the phagosome pathway was also significantly enriched, with the expression of *ATP6V0D2* and *ATP6V0A4* markedly up-regulated. *ATP6V0D2* is a component of the V-ATPase complex, which plays a critical role in maintaining the acidic environment of organelles, such as lysosome, by pumping protons into these compartments. This low pH environment is essential for the activity of hydrolytic enzymes that degrade various substrates within the lysosome (Vasanthakumar and Rubinstein, 2020). Furthermore, *ATP6V0D2* facilitates the fusion of autophagosomes and lysosomes during autophagy, enabling the degradation of unnecessary or damaged cellular components and ensuring the smooth progression of the autophagy (Xia et al., 2019). In the present study, the results of IHC staining showed that compared with APEC infection alone, the expression of p62 protein was significantly reduced, and LC-3II protein expression showed an increasing trend in CORT pretreatment followed APEC infection broilers, indicating that the degree of autophagy was increased. Additionally, we observed that the PPAR signaling pathway was significantly enriched. The up-regulation of *PCK1* and down-regulation of *PLIN1* suggested that lipids in the liver were more likely to be degraded (Ye et al., 2023). Studies have shown that lipids not only act as energy storage molecules, but also as signaling molecules to regulate the function of immune cells (Fan et al., 2023; Tan et al., 2023; Zheng et al., 2024). Fan et al. found that LPS treatment of murine hepatic Kupffer cells led to an increase in intracellular lipid droplets accumulation, resulting in increased lysophosphatidic acid content, which promoted the release of pro-inflammatory cytokines by Kupffer cells and finally led to mitochondrial dysfunction (Fan et al., 2023). However, in pigs infected with porcine reproductive and respiratory syndrome virus (**PRRSV**), Yin Yang 1 (**YY1**) positively regulated the expression of *PPAR-γ* to promote the synthesis of lipid droplets, thus inhibiting PRRSV replication (Zheng et al., 2024). In the present study, CORT treatment induced an increased proportion of lipid droplets in the liver, and such an alteration may be involved in the response to subsequent APEC infection. The above results suggest that CORT pretreatment followed by APEC infection enhances the cellular self-renewal and clearance capacity, alleviating hepatocyte apoptosis, with lipids potentially playing a role in this process.

GR is expressed in almost all cell types. Upon phosphorylation and nuclear translocation, it can induce or suppress the expression of numerous genes, regulating a wide range of biological processes, including metabolism, development, cognition, and immunity (Quatrini and Ugolini, 2020). When combined with glucocorticoid, GR inhibits the expression of transcription factors AP-1 and NF-κB, which are major downstream effectors of proinflammatory signaling pathways (Quax et al., 2013). In T cells, GR binds to the PD-1 promoter, thereby promoting the transcription of PD-1. Under normal conditions, PD-1 expression contributes to the regulation of immune responses. However, in the tumor microenvironment, sustained activation of PD-1 leads to T cell dysfunction, rendering them unable to effectively kill tumor cells (Maeda et al., 2019). In the present study, the results showed that CORT treatment and APEC infection both led to increased p-GR protein expression. However, compared with APEC infection alone, pretreatment with CORT followed by APEC infection significantly reduced the p-GR protein expression in liver. Therefore, we speculated that GR may play a certain regulatory role in gene expression. Furthermore, we utilized an online database to predict target genes of GR and performed KEGG pathway analysis. The results were compared with the KEGG pathway analysis of liver RNA-Seq data. Overlapping pathways identified between the two analyses included cytokine-cytokine receptor interaction pathway, PPAR signaling pathway, p53 signaling pathway, phagosome pathway and other pathways. Moreover, the DEGs in these pathways in RNA-Seq were precisely the predicted target genes of GR, suggesting that GR may regulate these biological processes by modulating the expression of these DEGs. However, whether and how GR regulates the expression of these genes needs to be verified.

Conclusion

In conclusion, our findings indicate that both CORT treatment and APEC infection impair broiler growth performance, affect immune function, cause liver injury, and remodel lipid metabolism. Additionally, CORT pretreatment followed by APEC infection enhances innate immune function of broilers and partially alleviates liver damage, with lipid metabolism likely play a key role in this process. These results provide a theoretical basis for improving poultry health management and disease prevention strategies.

Conflict of interest

This manuscript is an original, unpublished work and has not been submitted to any other journals for publication, in whole or in part. All authors listed have read and approved this manuscript, and there is no conflict of interest in the submission of this manuscript.

Acknowledgements

This work was supported by the Biological Breeding-National Science and Technology Major Project (2023ZD0405305). Thanks to Jiangsu Lihua Animal Husbandry Co., LTD. for providing avian pathogenic *Escherichia coli* O18 strain.

Disclosures

This manuscript is an original, unpublished work and has not been submitted to any other journals for publication, in whole or in part. All authors listed have read and approved this manuscript, and there is no conflict of interest in the submission of this manuscript.

Supplementary materials

Supplementary material associated with this article can be found, in the online version, at doi:10.1016/j.psj.2025.105020.

References

Bailey, M.T., Engler, H., Powell, N.D., Padgett, D.A., Sheridan, J.F., 2007. Repeated social defeat increases the bactericidal activity of splenic macrophages through a toll-like receptor-dependent pathway. Am. J. Physiol. Regul. Integr. Comp. Physiol. 293 (3), R1180–R1190.

Bekhbat, M., Rowson, S.A., Neigh, G.N., 2017. Checks and balances: the glucocorticoid receptor and NFκB in good times and bad. Front. Neuroendocrinol. 46, 15–31.

Bélanger, L., Garenaux, A., Harel, J., Boulianne, M., Nadeau, E., Dozois, C.M., 2011. *Escherichia coli* from animal reservoirs as a potential source of human extraintestinal pathogenic *E.coli*. FEMS Immunol. Med. Microbiol. 62 (1), 1–10.

Cao, Z., Ma, B., Cui, C., Zhao, J., Liu, S., Qiu, Y., Zheng, Y., Gao, M., Luan, X., 2022. Protective effects of AdipoRon on the liver of Huoyan goose fed a high-fat diet. Poult. Sci. 101 (4), 101708.

Chrousos, G.P., Gold, P.W., 1992. The concepts of stress and stress system disorders. Overview of physical and behavioral homeostasis. Jama 267 (9), 1244–1252.

Cruvinel, J.M., Groff Urayama, P.M., Oura, C.Y., de Lima Krenchinski, F.K., dos Santos, T. S., de Souza, B.A., Kadri, S.M., Correa, C.R., Sartori, J.R., Pezzato, A.C., 2023. Pequi oil (Caryocar brasiliense Camb.) attenuates the adverse effects of cyclical heat stress and modulates the oxidative stress-related genes in broiler chickens. Animals(Basel) 13 (12), 1896.

Dai, J., Wang, H., Liao, Y., Tan, L., Sun, Y., Song, C., Liu, W., Ding, C., Luo, T., Qiu, X., 2022. Non-targeted metabolomic analysis of chicken kidneys in response to coronavirus IBV infection under stress induced by dexamethasone. Front. Cell. Infect. Microbiol. 12, 945865.

Duan, Y., Fu, W., Wang, S., Ni, Y., Zhao, R., 2014. Effects of tonic immobility (TI) and corticosterone (CORT) on energy status and protein metabolism in pectoralis major muscle of broiler chickens. Comp. Biochem. Physiol. A: Mol. Integr. Physiol. 169, 90–95.

Dziva, F., Stevens, M.P., 2008. Colibacillosis in poultry: unravelling the molecular basis of virulence of avian pathogenic *Escherichia coli* in their natural hosts. Avian Pathol. 37 (4), 355–366.

El-Shenawy, F.A., El-Sherbeny, E.M.E., Kassem, S., 2023. Efficacy of zinc oxide and copper oxide nanoparticles on virulence genes of avian pathogenic *E. coli* (APEC) in broilers. BMC Vet. Res. 19 (1), 108.

Fan, G., Li, Y., Zong, Y., Suo, X., Jia, Y., Gao, M., Yang, X., 2023. GPAT3 regulates the synthesis of lipid intermediate LPA and exacerbates Kupffer cell inflammation mediated by the ERK signaling pathway. Cell. Death Dis. 14 (3), 208.

Gjerstad, J.K., Lightman, S.L., Spiga, F., 2018. Role of glucocorticoid negative feedback in the regulation of HPA axis pulsatility. Stress 21 (5), 403–416.

Guan, Z.H., Yang, D., Wang, Y., Ma, J.B., Wang, G.N., 2024. Ectodysplasin-A2 receptor (EDA2R) knockdown alleviates myocardial ischemia/reperfusion injury through inhibiting the activation of the NF-κB signaling pathway. Exp. Anim. 73 (4), 376–389.

Guo, Z., Wu, Q., Xie, P., Wang, J., Lv, W., 2024. Immunomodulation in non-alcoholic fatty liver disease: exploring mechanisms and applications. Front. Immunol. 15, 1336493.

Ha, E.J., Hong, S.M., Kim, S.J., Ahn, S.M., Kim, H.W., Choi, K.S., Kwon, H.J., 2023. Tracing the evolutionary pathways of serogroup O78 avian pathogenic *Escherichia coli*. Antibiotics (Basel) 12 (12), 1714.

2nd Helmy, Y.A., Kathayat, D., Deblais, L., Srivastava, V., Closs Jr., G., Tokarski, R.J., Ayinde, O., Fuchs, J.R., Rajashekara, G., 2022. Evaluation of novel quorum sensing inhibitors targeting auto-inducer 2 (AI-2) for the control of avian pathogenic *Escherichia coli* infections in chickens. Microbiol. Spectr. 10 (3), e0028622.

Heymann, F., Tacke, F., 2016. Immunology in the liver-from homeostasis to disease. Nat. Rev. Gastroenterol. Hepatol. 13 (2), 88–110.

Hu, J., Afayibo, D.J.A., Zhang, B., Zhu, H., Yao, L., Guo, W., Wang, X., Wang, Z., Wang, D., Peng, H., Tian, M., Qi, J., Wang, S., 2022. Characteristics, pathogenic mechanism, zoonotic potential, drug resistance, and prevention of avian pathogenic *Escherichia coli* (APEC). Front. Microbiol. 13, 1049391.

Hu, Q., Zhang, T., He, H., Pu, F., Zhang, R., Li, L., Hu, J., Bai, L., Han, C., Wang, J., Liu, H., 2024. Impacts of longitudinal water curtain cooling system on transcriptome-related immunity in ducks. BMC Genom. 25 (1), 333.

Hu, Y., Sun, Q., Hu, Y., Hou, Z., Zong, Y., Omer, N.A., Abobaker, H., Zhao, R., 2018. Corticosterone-induced lipogenesis activation and lipophagy inhibition in chicken liver are alleviated by maternal betaine supplementation. J. Nutr. 148 (3), 316–325.

Islam, R., Sultana, N., Haque, Z., Islam, M.R., 2023. Effect of dietary dexamethasone on the morphologic and morphometric adaptations in the lymphoid organs and mortality rate in broilers. Vet. Med. Sci. 9 (4), 1656–1665.

Jiang, Z., Luo, M., Ma, W., Ma, S., Wang, Y., Zhang, K., 2021. Protective effects of 1,8-cineole microcapsules against inflammation and gut microbiota imbalance associated weight loss induced by heat stress in broiler chicken. Front. Pharmacol. 11, 585945.

Kathayat, D., Lokesh, D., Ranjit, S., Rajashekara, G., 2021. Avian pathogenic *Escherichia coli* (APEC): an overview of virulence and pathogenesis factors, zoonotic potential, and control strategies. Pathogens 10 (4), 467.

Kim, D.Y., Kim, J.H., Choi, W.J., Han, G.P., Kil, D.Y., 2021. Comparative effects of dietary functional nutrients on growth performance, meat quality, immune responses, and stress biomarkers in broiler chickens raised under heat stress conditions. Anim. Biosci. 34 (11), 1839–1848.

Korbecki, J., Grochans, S., Gutowska, I., Barczak, K., Baranowska-Bosiacka, I., 2020. CC chemokines in a tumor: a review of pro-cancer and anti-cancer properties of receptors CCR5, CCR6, CCR7, CCR8, CCR9, and CCR10 ligands. Int. J. Mol. Sci. 21, 7619, 20.

Krishnan, S., Chang, A.C., Hodges, J., Couraud, P.-O., Romero, I.A., Weksler, B., Nicholson, B.A., Nolan, L.K., Prasadarao, N.V., 2015. Serotype O18 avian pathogenic and neonatal meningitis *Escherichia coli* strains employ similar pathogenic strategies for the onset of meningitis. Virulence 6 (8), 777–786.

Li, J., Wang, X., Ackerman, W.E., Batty, A.J., Kirk, S.G., White, W.M., Wang, X., Anastasakis, D., Samavati, L., Buhimschi, I., Nelin, L.D., Hafner, M., Liu, Y., 2018. Dysregulation of lipid metabolism in Mkp-1 deficient mice during gram-negative sepsis. Int. J. Mol. Sci. 19 (12), 3904.

Li, Z., Liu, A., Xu, J., Zhang, C., 2023. Resveratrol attenuates heat-stress-impaired immune and inflammatory responses of broilers by modulating toll-like receptor-4 signaling pathway. Braz. J. Poultry Sci. 25 (2).

Liu, J., Zhang, K., Zhao, M., Chen, L., Chen, H., Zhao, Y., Zhao, R., 2024. Dietary bile acids alleviate corticosterone-induced fatty liver and hepatic glucocorticoid receptor suppression in broiler chickens. J. Anim. Sci. 102, skae338.

Liu, Y., Liu, Z., Xing, T., Li, J., Zhang, L., Zhao, L., Gao, F., 2023. Effect of chronic heat stress on the carbonylation of glycolytic enzymes in breast muscle and its correlation with the growth performance of broilers. Poult. Sci. 102 (12), 103103.

Luo, J.J., Chen, W., Qu, H., Liu, Y.Q., Luo, C.L., Ji, J., Shu, D.M., Wang, J., 2022. Dietary supplementation with yucca alleviates heat stress in growing broilers exposed to high ambient temperature. Front. Vet. Sci. 9, 850715.

Maeda, N., Maruhashi, T., Sugiura, D., Shimizu, K., Okazaki, I.M., Okazaki, T., 2019. Glucocorticoids potentiate the inhibitory capacity of programmed cell death 1 by up-regulating its expression on T cells. J. Biol. Chem. 294 (52), 19896–19906.

Mao, N., Yu, Y., Cui, J., He, J., Yang, Y., Wang, D., 2024. Effect of matrine on growth performance, gut health, and gut microbiota in chickens infected with avian pathogenic *Escherichia coli*. Poult. Sci. 104 (1), 104520.

Mehaisen, G.M.K., Eshak, M.G., El Sabry, M.I., Abass, A.O., 2016. Expression of inflammatory and dell death program genes and comet DNA damage assay induced by Escherichia coli in layer hens. PLoS. One 11 (6), e0158314.

Mehat, J.W., van Vliet, A.H.M., La Ragione, R.M., 2021. The avian pathogenic *Escherichia coli* (APEC) pathotype is comprised of multiple distinct, independent genotypes. Avian Pathol. 50 (5), 402–416.

Mellata, M., 2013. Human and avian extraintestinal pathogenic *Escherichia coli*: infections, zoonotic risks, and antibiotic resistance trends. Foodborne Pathog. Dis. 10 (11), 916–932.

Meng, J., Wang, W., Ding, J., Gu, B., Zhou, F., Wu, D., Fu, X., Qiao, M., Liu, J., 2024. The synergy effect of matrine and berberine hydrochloride on treating colibacillosis caused by an avian highly pathogenic multidrug-resistant *Escherichia coli*. Poult. Sci. 103 (10), 104151.

Mohammed, A.A., Jiang, S., Jacobs, J.A., Cheng, H.W., 2019. Effect of a synbiotic supplement on cecal microbial ecology, antioxidant status, and immune response of broiler chickens reared under heat stress. Poult. Sci. 98 (10), 4408–4415.

Nihashi, Y., Ono, T., Kagami, H., Takaya, T., 2019. Toll-like receptor ligand-dependent inflammatory responses in chick skeletal muscle myoblasts. Dev. Comp. Immunol. 91, 115–122.

Quatrini, L., Ugolini, S., 2020. New insights into the cell- and tissue-specificity of glucocorticoid actions. Cell. Mol. Immunol. 18 (2), 269–278.

Quax, R.A., Manenschijn, L., Koper, J.W., Hazes, J.M., Lamberts, S.W., van Rossum, E.F., Feelders, R.A., 2013. Glucocorticoid sensitivity in health and disease. Nat. Rev. Endocrinol. 9 (11), 670–686.

Quinteiro-Filho, W.M., Gomes, A.V.S., Pinheiro, M.L., Ribeiro, A., Ferraz-de-Paula, V., Astolfi-Ferreira, C.S., Ferreira, A.J.P., Palermo-Neto, J., 2012. Heat stress impairs

performance and induces intestinal inflammation in broiler chickens infected with *Salmonella Enteritidis*. Avian Pathol. 41 (5), 421–427.
Robinson, M.W., Harmon, C., O'Farrelly, C., 2016. Liver immunology and its role in inflammation and homeostasis. Cell. Mol. Immunol. 13 (3), 267–276.
Ruan, M.-L., Wang, J., Xia, Z.-Y., Li, X.-W., Zhang, B., Wang, G.-L., Wu, Y.-Y., Han, Y., Deng, J., Sun, L.-H., 2023. An integrated mycotoxin-mitigating agent can effectively mitigate the combined toxicity of AFB1, DON and OTA on the production performance, liver and oviduct health in broiler breeder hens. Food Chem. Toxicol. 182, 114159.
Su, Y., Qu, Q., Li, J., Han, Z., Fang, Y., Flavorta, B.L., Jia, Z., Yu, Q., Zhang, Y., Qian, P., Tang, X., 2024. Perilipin1 inhibits *Nosema bombycis* proliferation by promoting *Domeless*- and *Hop*-mediated JAK-STAT pathway activation in *Bombyx mori*. Microbiol. Spectr. 12 (6), e0367123.
Tan, Y.j., Jin, Y., Zhou, J., Yang, Y.f., 2023. Lipid droplets in pathogen infection and host immunity. Acta Pharmacol. Sin. 45 (3), 449–464.
Tan, Z., Chen, Y., Zhou, Y., 2024b. Palygorskite improves growth performance and prevents liver damage in avian pathogenic *Escherichia coli*-challenged broiler chickens at an early age. J. Anim. Sci. 102, skae302.
Tan, Z., Chen, Y., Wen, C., Zhou, Y., 2024a. Dietary supplementation with a silicate clay mineral (palygorskite) alleviates inflammatory responses and intestinal barrier damage in broiler chickens challenged with *Escherichia coli*. Poult. Sci. 103 (9), 104017.
Tang, L.P., Li, W.H., Liu, Y.L., Lun, J.C., He, Y.M., 2021. Heat stress inhibits expression of the cytokines, and NF-κB-NLRP3 signaling pathway in broiler chickens infected with *salmonella typhimurium*. J. Therm. Biol. 98, 102945.
Thiam, M., Wang, Q., Barreto Sánchez, A.L., Zhang, J., Ding, J., Wang, H., Zhang, Q., Zhang, N., Wang, J., Li, Q., Wen, J., Zhao, G., 2022. Heterophil/lymphocyte ratio level modulates *Salmonella* resistance, cecal microbiota composition and functional capacity in infected chicken. Front. Immunol. 13, 816689.
Vasanthakumar, T., Rubinstein, J.L., 2020. Structure and roles of V-type ATPases. Trends Biochem. Sci. 45 (4), 295–307.
Xia, Y., Liu, N., Xie, X., Bi, G., Ba, H., Li, L., Zhang, J., Deng, X., Yao, Y., Tang, Z., Yin, B., Wang, J., Jiang, K., Li, Z., Choi, Y., Gong, F., Cheng, X., O'Shea, J.J., Chae, J.J., Laurence, A., Yang, X.-P., 2019. The macrophage-specific V-ATPase subunit ATP6V0D2 restricts inflammasome activation and bacterial infection by facilitating autophagosome-lysosome fusion. Autophagy 15 (6), 960–975.
Ye, Q., Liu, Y., Zhang, G., Deng, H., Wang, X., Tuo, L., Chen, C., Pan, X., Wu, K., Fan, J., Pan, Q., Wang, K., Huang, A., Tang, N., 2023. Deficiency of gluconeogenic enzyme PCK1 promotes metabolic-associated fatty liver disease through PI3K/AKT/PDGF axis activation in male mice. Nat. Commun. 14 (1), 1402.
Zhang, G., Sunkara, L., 2014. Avian antimicrobial host defense peptides: from biology to therapeutic applications. Pharmaceuticals 7 (3), 220–247.
Zhang, H., Coblentz, C., Watanabe-Smith, K., Means, S., Means, J., Maxson, J.E., Tyner, J.W., 2018. Gain-of-function mutations in granulocyte colony–stimulating factor receptor (CSF3R) reveal distinct mechanisms of CSF3R activation. J. Biol. Chem. 293 (19), 7387–7396.
Zhang, Y., Wang, L., Shao, J., Liu, Y., Lu, Y., Yang, J., Xu, S., Zhang, J., Li, M., Liu, X., Zheng, M., 2023. Nano-calcipotriol as a potent anti-hepatic fibrosis agent. MedComm 4 (5), e354, 2020.
Zheng, Z., Ling, X., Li, Y., Qiao, S., Zhang, S., Wu, J., Ma, Z., Li, M., Guo, X., Li, Z., Feng, Y., Liu, X., Goodfellow, I.G., Zheng, H., Xiao, S., 2024. Host cells reprogram lipid droplet synthesis through YY1 to resist PRRSV infection. mBio 15, e0154924, 8.
Zhu, Y., Kubota, S., Pasri, P., Rakngam, S., Okrathok, S., Pukkung, C., Yang, S., Khempaka, S., 2024. Transcriptome analysis of jejunal mucosal tissue in breeder hens exposed to acute heat stress. Poult. Sci. 104 (1), 104532.